Electroexcitation of Nucleon Resonances with CLAS and Beyond

Ralf W. Gothe

UNIVERSITY OF SOUTH CAROLINA

NSTAR2026

September 7-11, 2026 Seville, Spain

- Why are $\gamma_v NN^*$ electrocouplings interesting? Probe bound valence quarks, baryon wave functions, the emergence of mass, and finally strong QCD.
- Experimental Foundation: Measure cross sections to reveal the space-time-dependent bound quark structure of baryons in various quantum configurations (I, J^π).
- Phenomenological Analyses / Theoretical Impact: Consistent extraction of $\gamma_v NN^*$ electrocouplings / mapping QCD continuously from sQCD towards pQCD.

This work is supported in parts by the National Science Foundation under Grant PHY 10014377.

Why is it Interesting?

Emergence of Hadron Mass Traced by Electromagnetic Probes

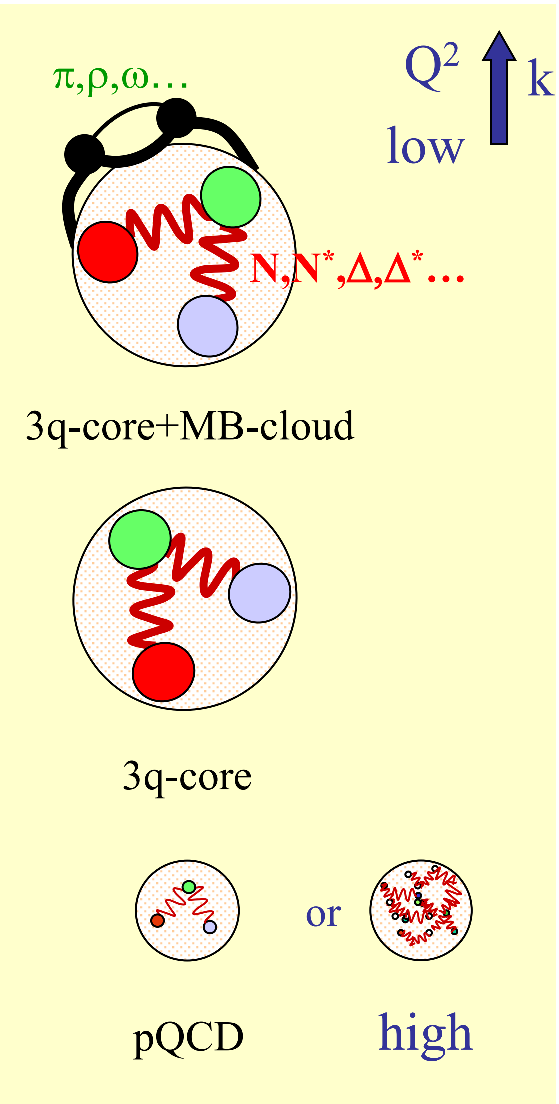

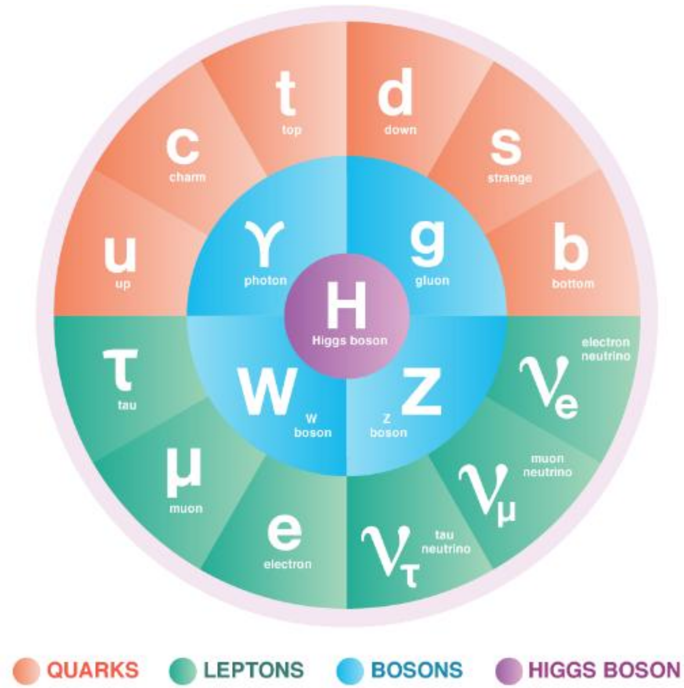

SM

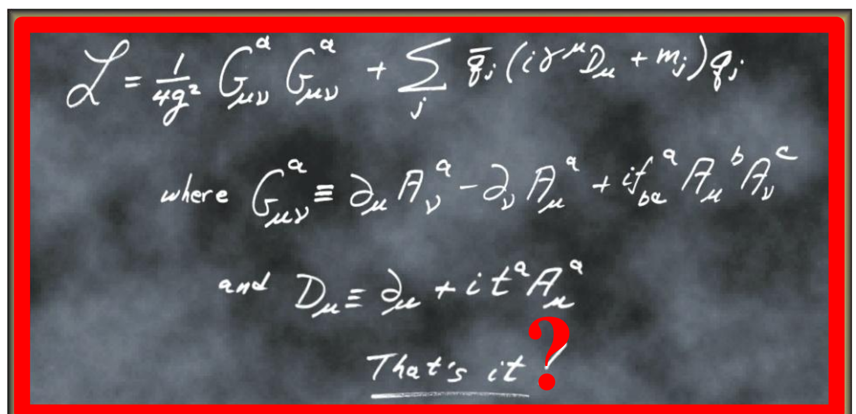

Frank Wilczek, Physics Today, August 2000

Hadron Structure with Electromagnetic Probes

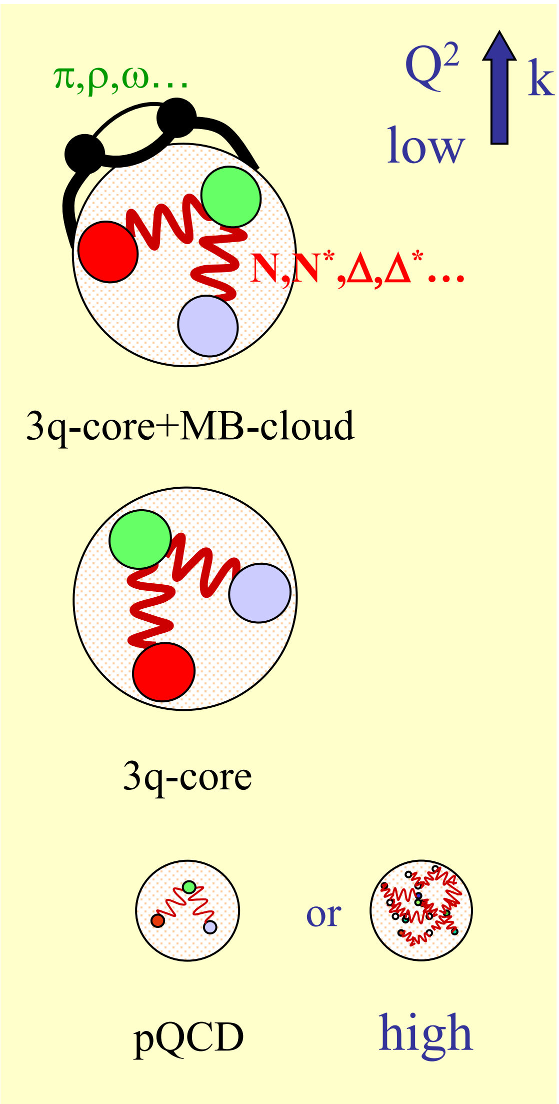

- The SM α_s diverges as Q^2 approaches zero, but confinement and the meson cloud heal this artificial divergence as QCD becomes non-perturbative.

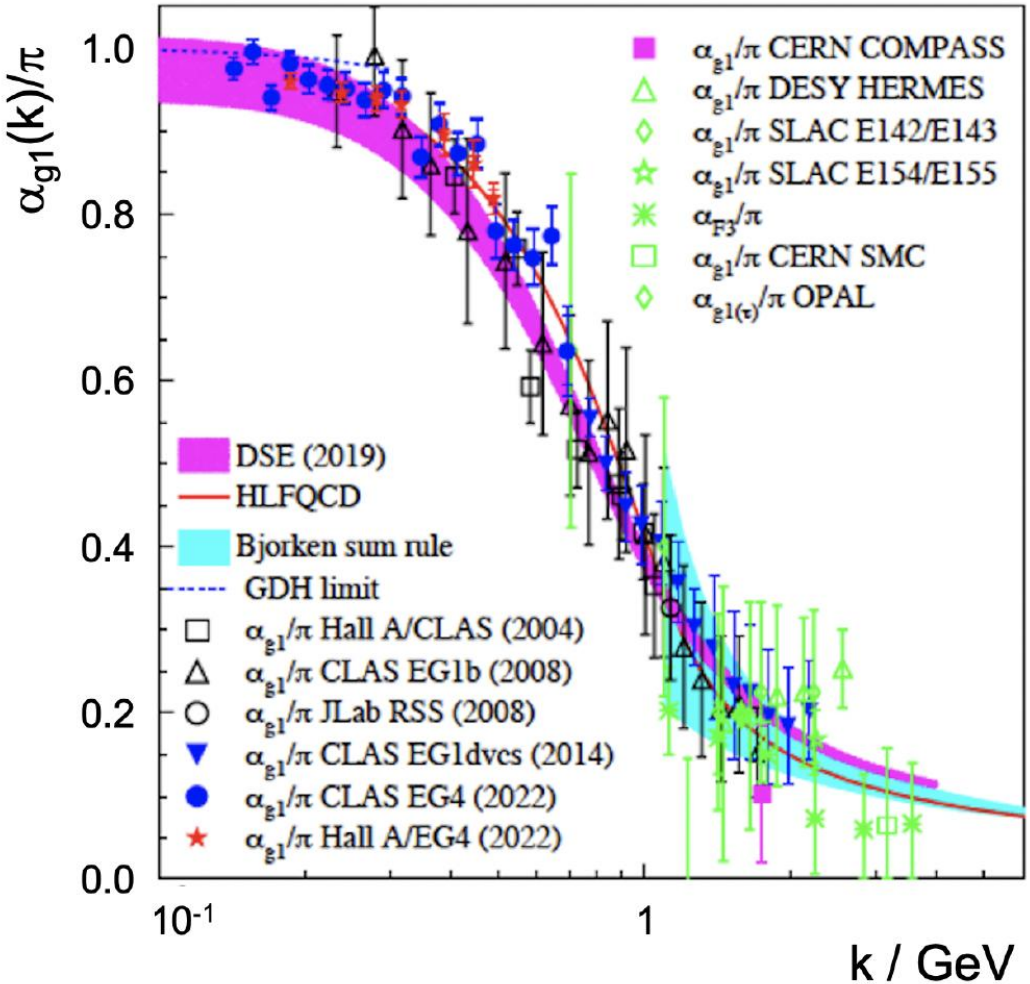

Hadron Structure with Electromagnetic Probes

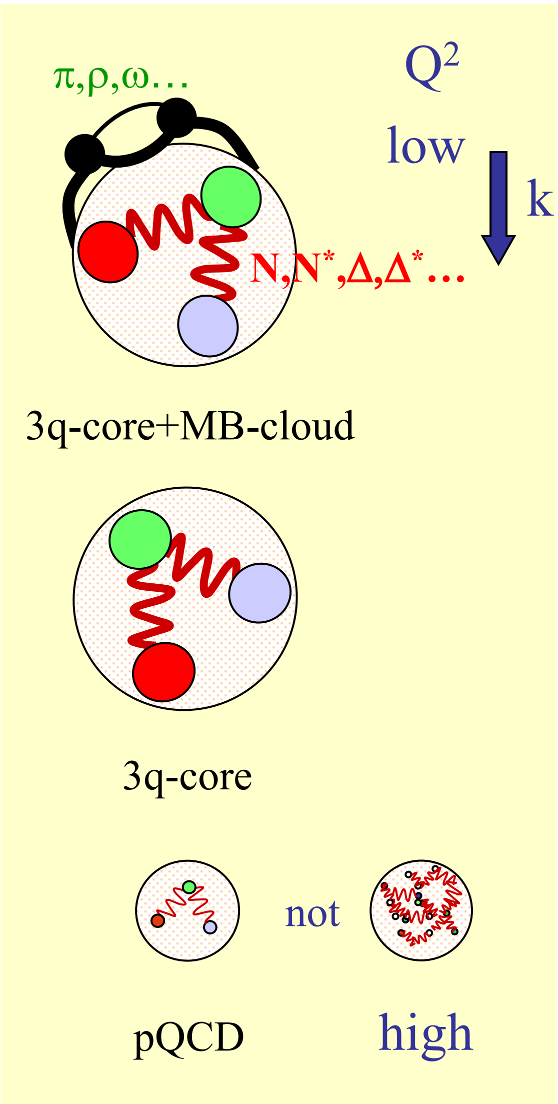

- Study the structure of the nucleon spectrum in the domain where dressed quarks are the major active degree of freedom.
- Explore the formation of excited nucleon states in interactions of dressed quarks at various distance scales and their emergence from QCD.

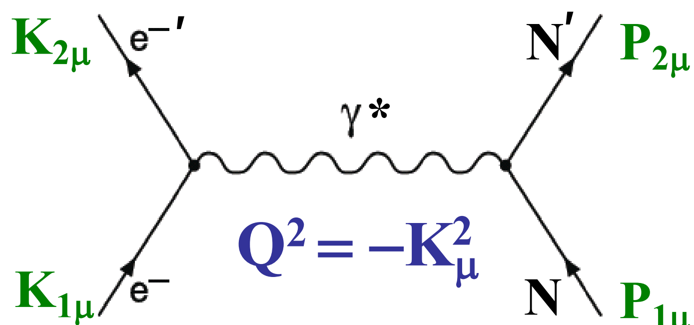

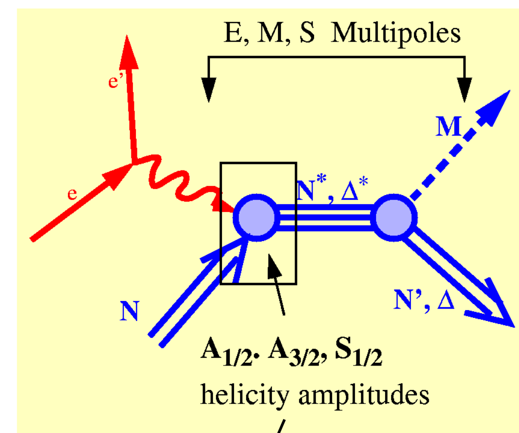

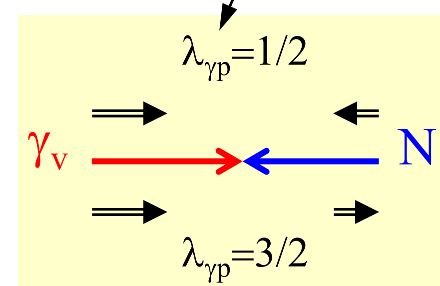

Probing pQCD Experimentally

How can one probe pQCD experimentally when measuring hadrons in the final state?

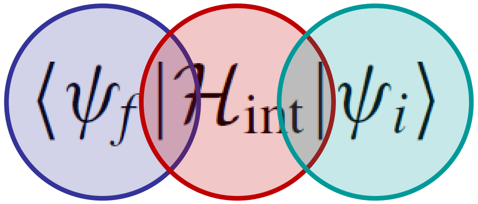

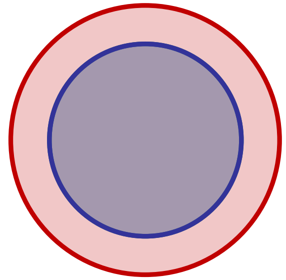

h^3 $\Delta E \to 0$ and $\Delta t \to \infty$

Elastic nuclear form factors

h^4

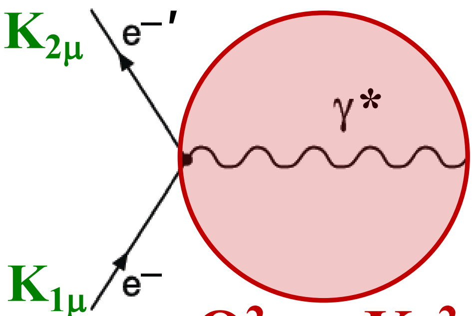

$Q^2 = -K_\mu{}^2$

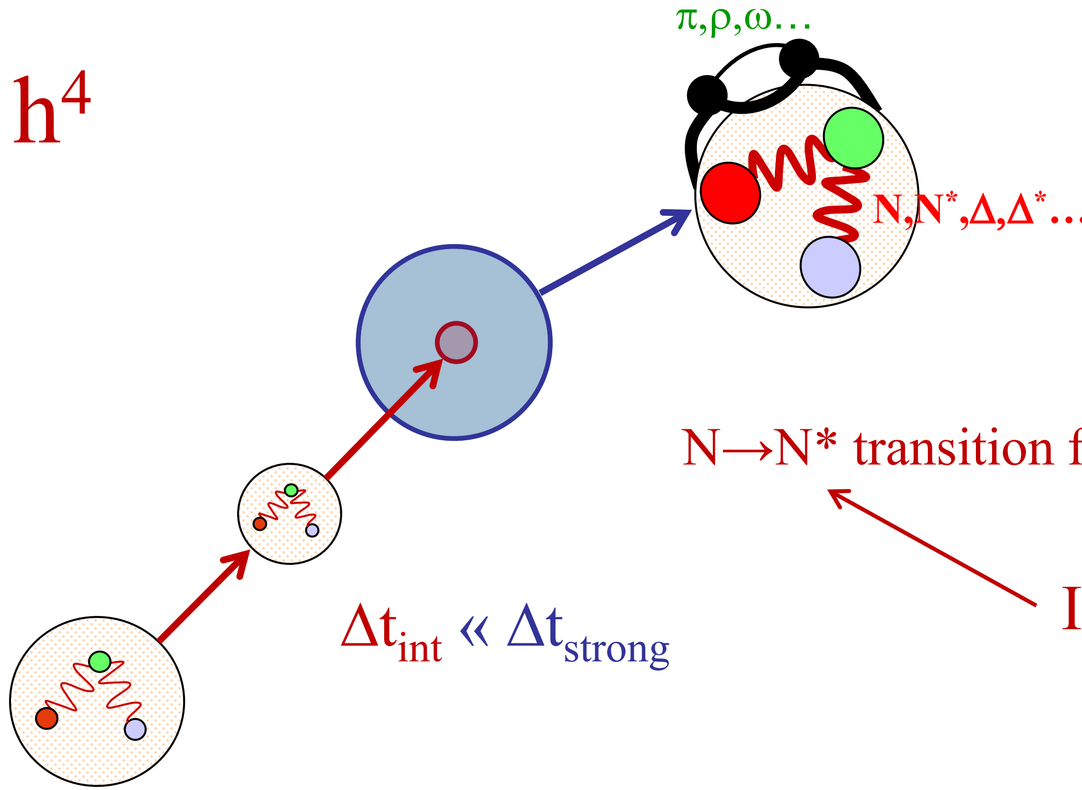

$N \to N^*$ transition form factors

$I,\ J^\pi$

$\Delta t_{int} \ll \Delta t_{strong}$

Structure Analysis of the Baryon

Demolition of a chimney at the "Henninger Brewery" in Frankfurt am Main, Germany, on 2 December 2006

hard and bound

hard and soft

hard and quasi-elastic

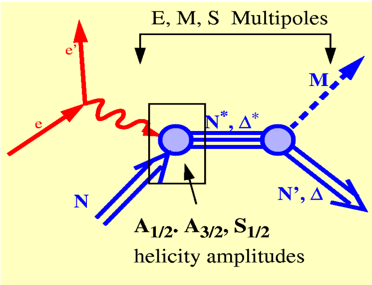

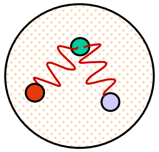

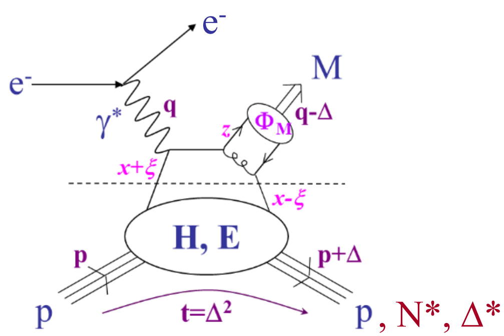

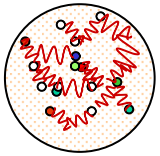

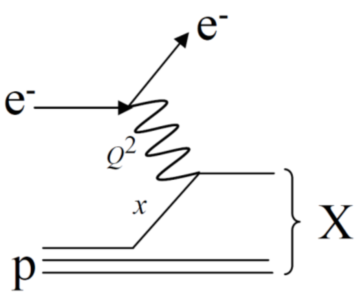

Structure Analysis of the Baryon

Demolition of a chimney at the "Henninger Brewery" in Frankfurt am Main, Germany, on 2 December 2006

hard and
bound

essence stays intact

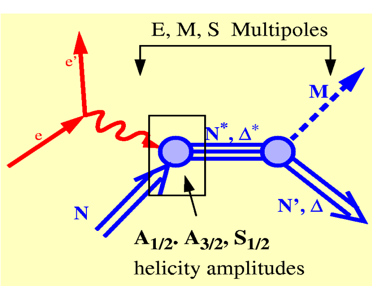

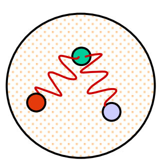

(I,J^{π})

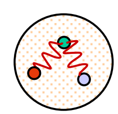

(I,J^{π})

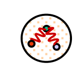

(I,J^{π})

Emergence of Hadron Mass Traced by Electromagnetic Probes

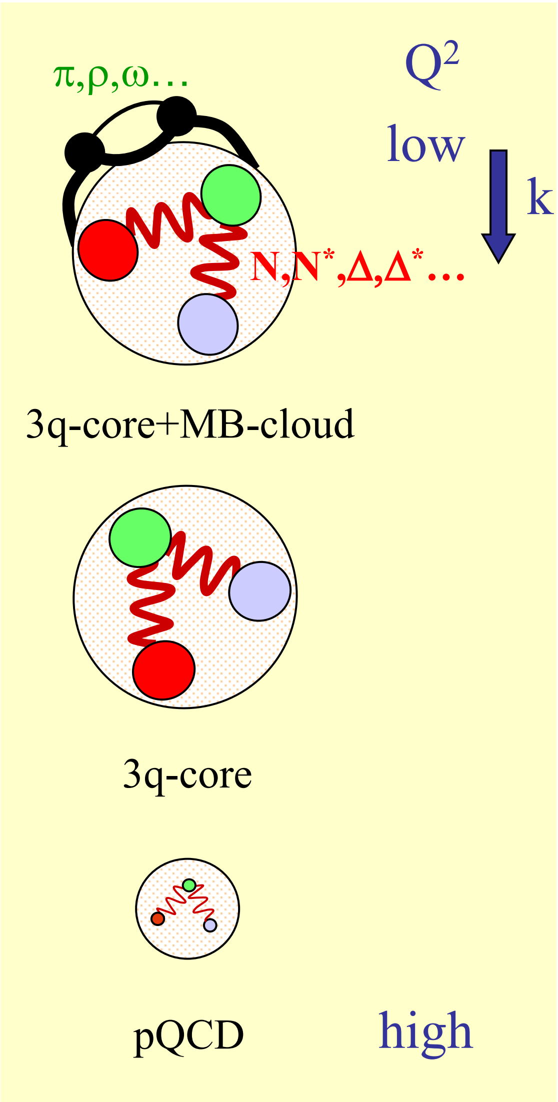

- Study the structure of the nucleon spectrum in the domain where dressed quarks are the major active degree of freedom.

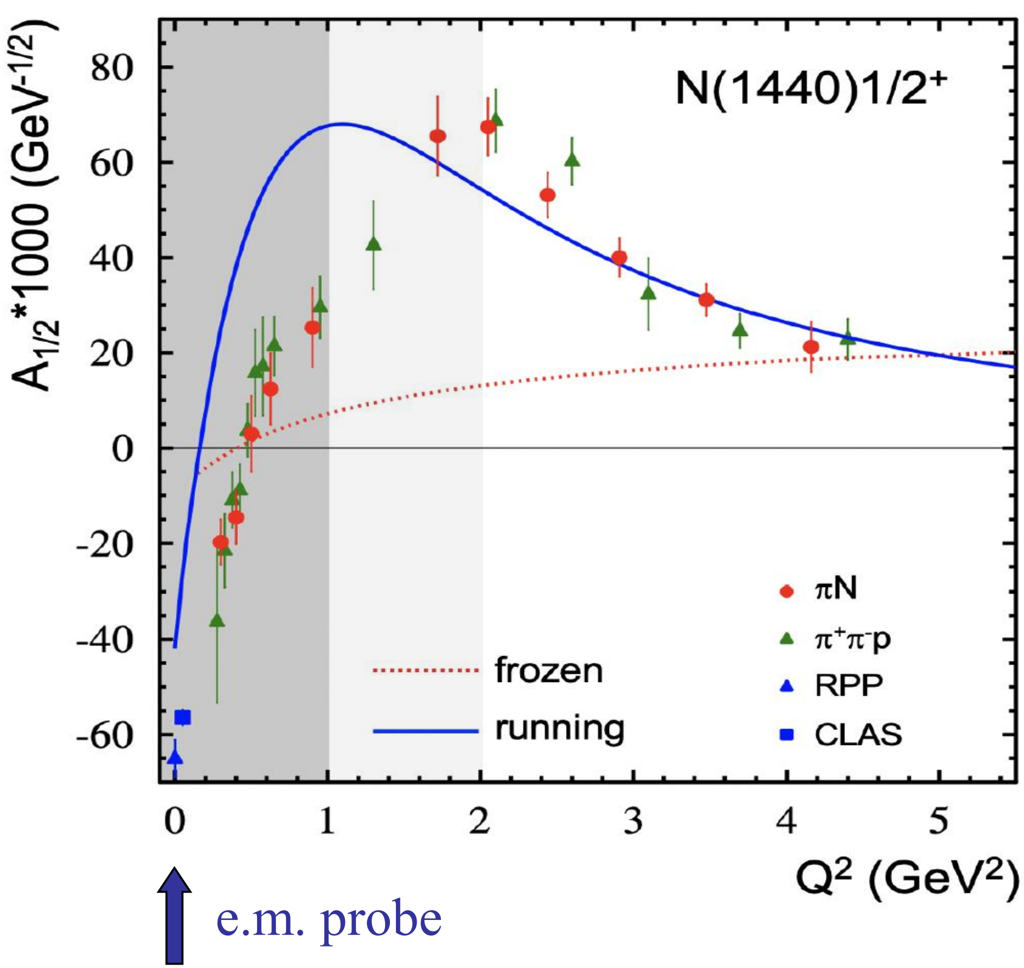

Emergence of Hadron Mass Traced by Electromagnetic Probes

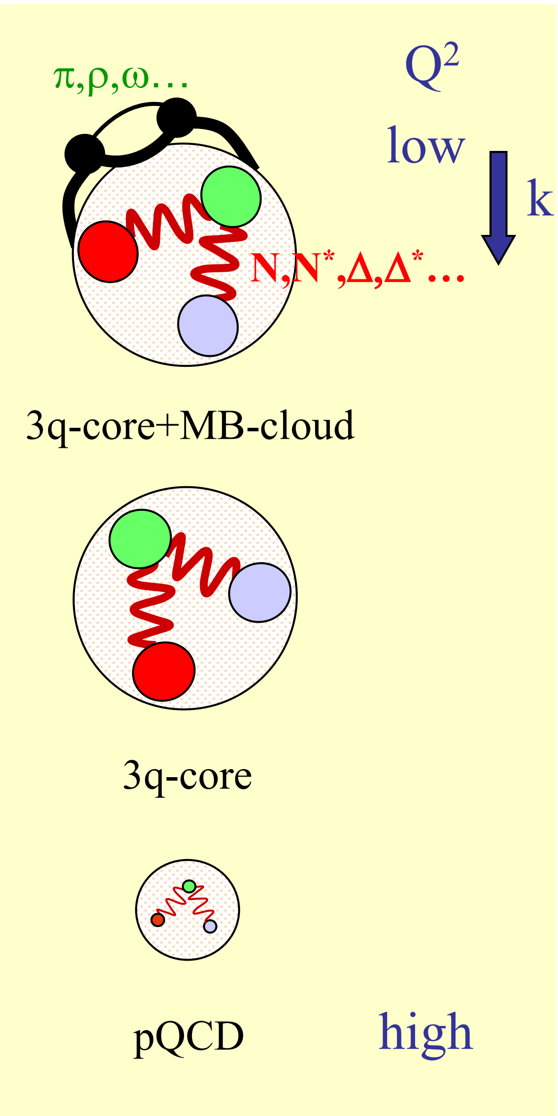

➢ Study the structure of the nucleon spectrum in the domain where most of the mass is generated by the strong field and dressed quarks are the major active degree of freedom.

Zhu-Fang Cui et al., Chin. Phys. C **44** (2020) 083102/1-10

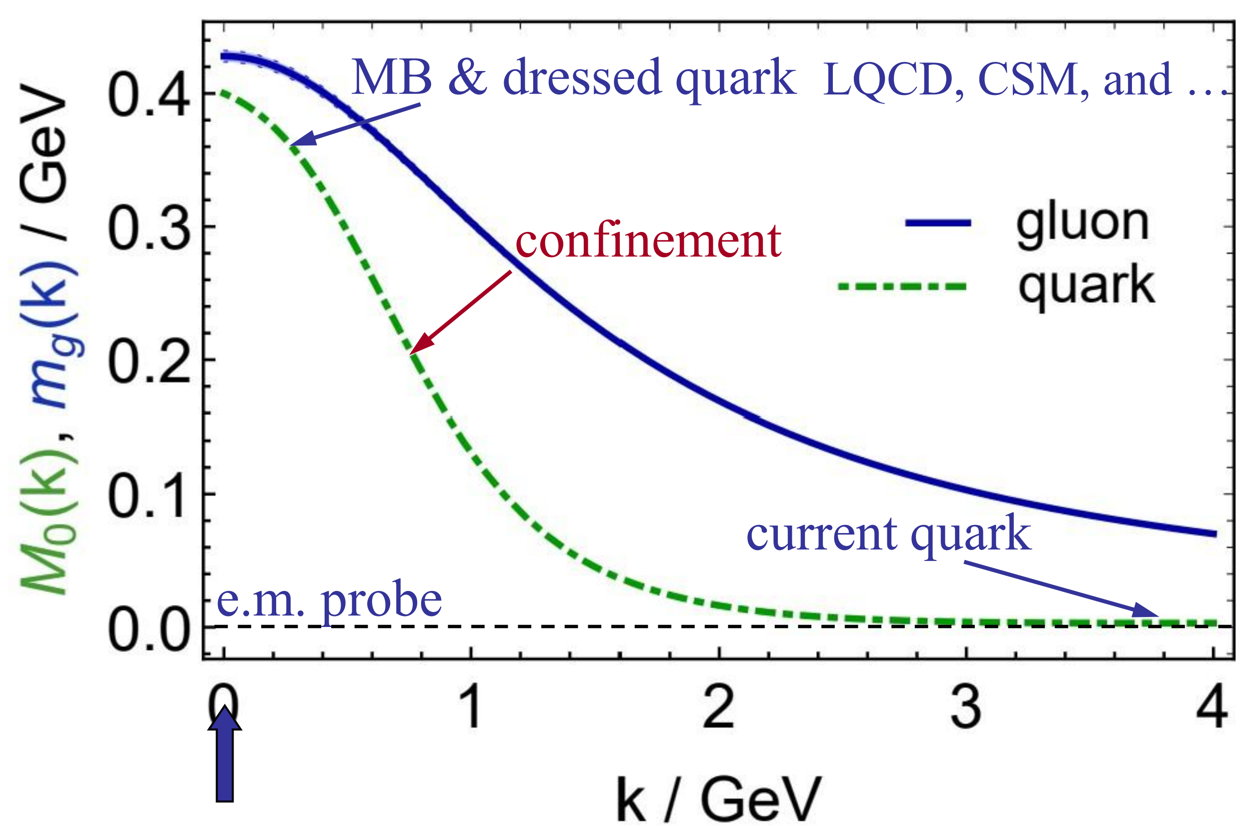

Experimental Foundation

Data-Driven Data Analyses

Consistent Results

Single Pion

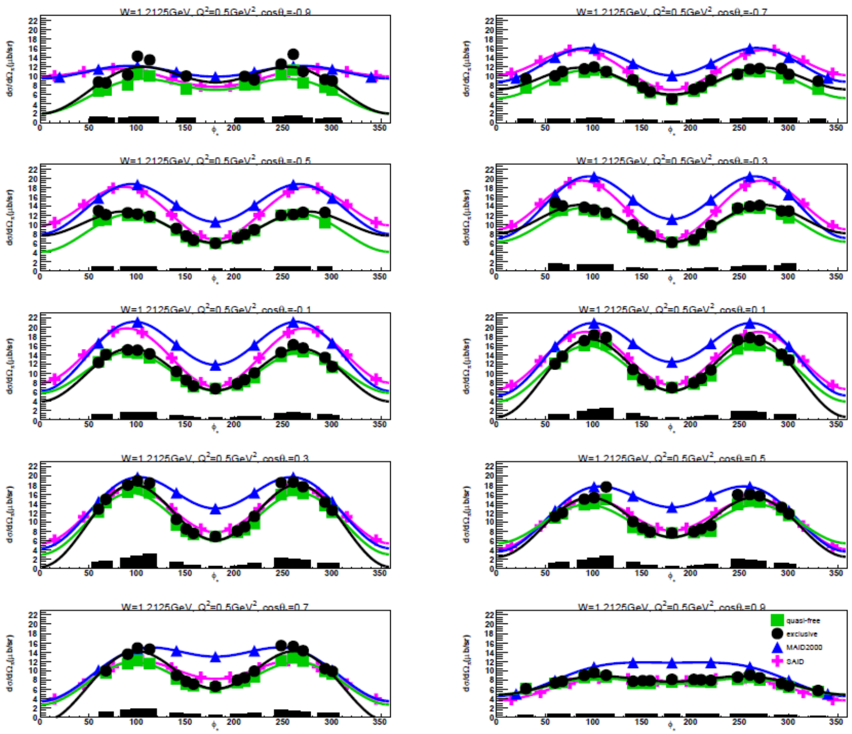

Y. Tian *et al.*, Phys. Rev. C 107, 015201 (2023) 26

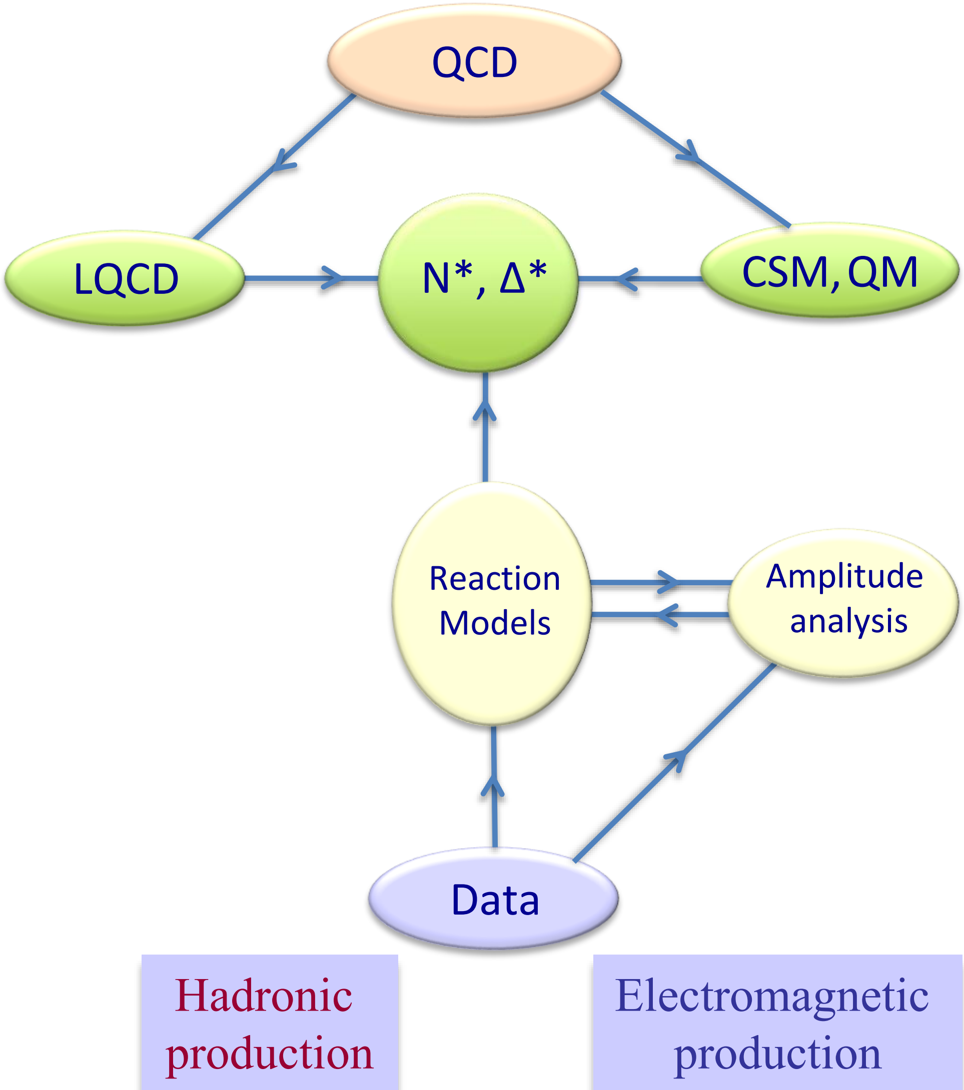

Exclusive Single π^- Electroproduction off the Deuteron

Ye Tian

$W = 1.2125$ GeV

$\Delta W = 25$ MeV

$Q^2 = 0.5$ GeV^2

$\Delta Q^2 = 0.2$ GeV^2

$\cos(\theta) = -0.7$

$\Delta\cos(\theta) = 0.2$

$\cos(\theta) = 0.9$

$\phi = 20^o$

$\Delta\phi = 40^o$

$\phi = 340^o$

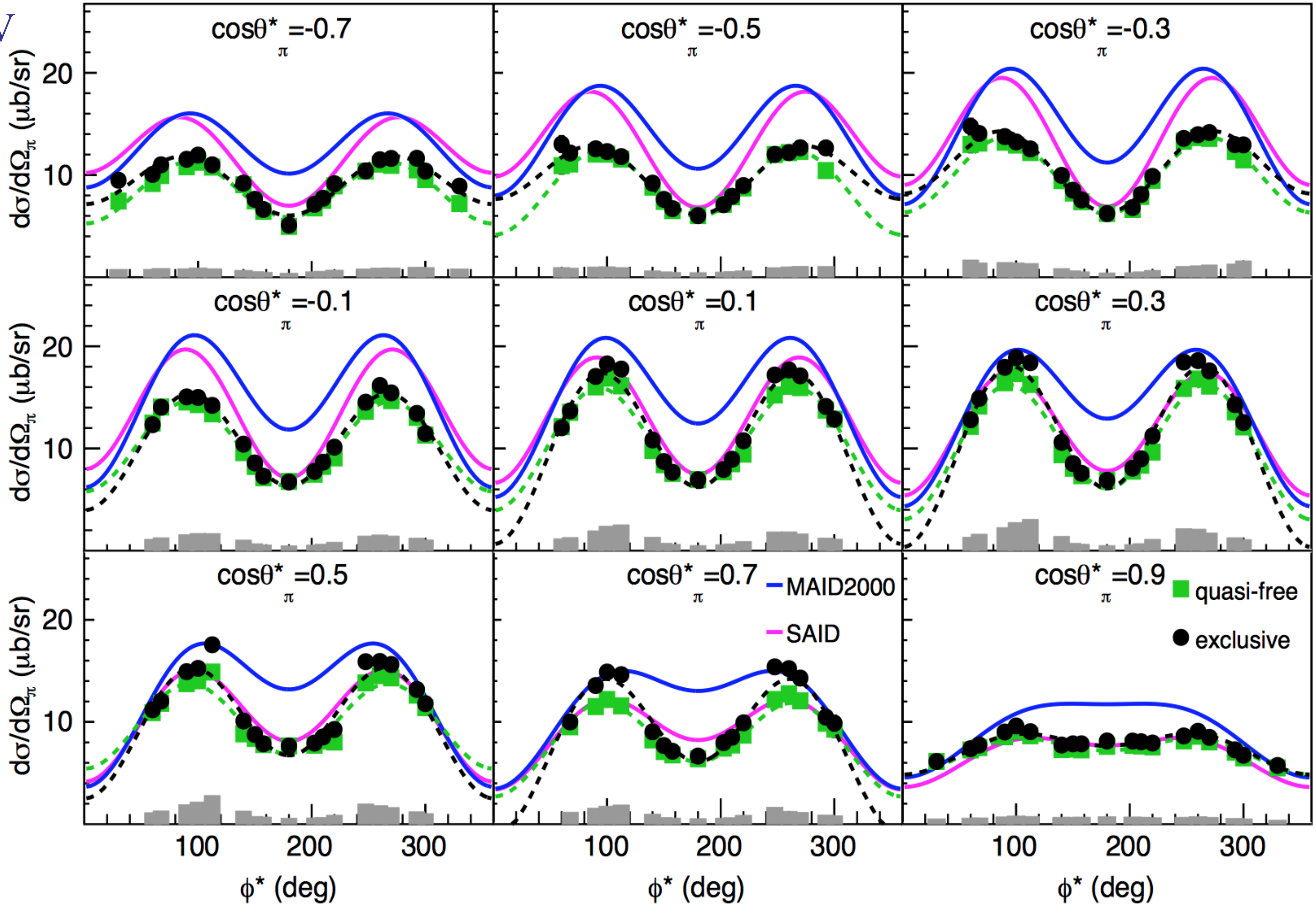

Exclusive Single π^- Electroproduction off the Deuteron

Ye Tian

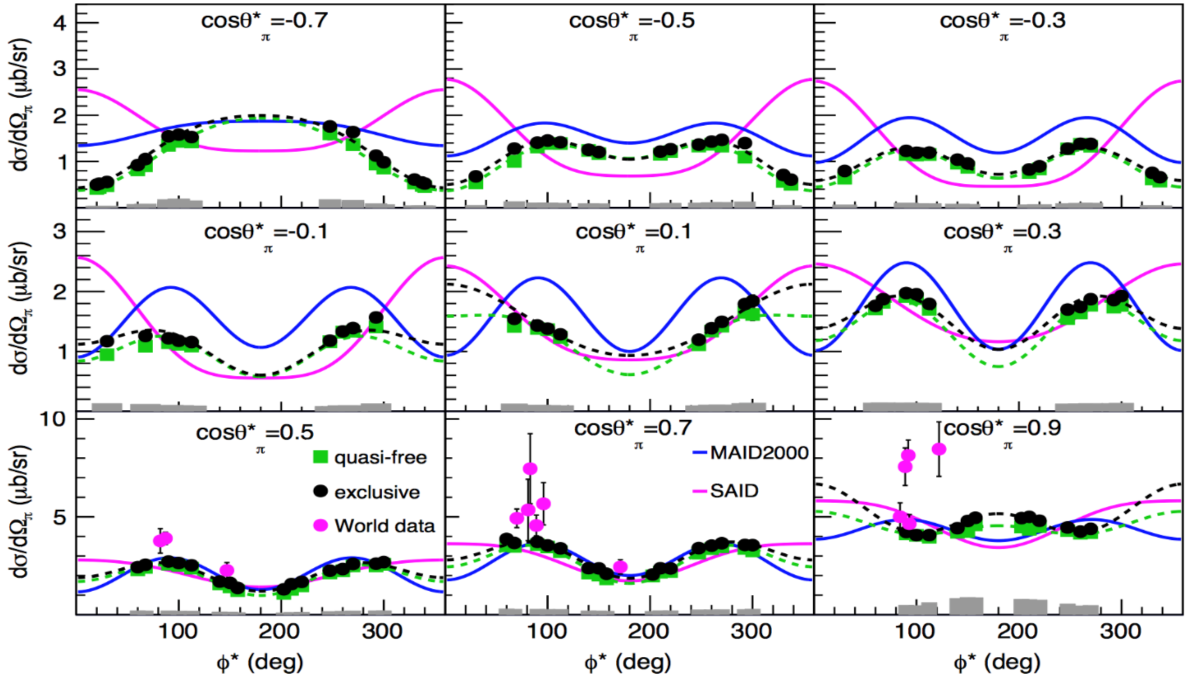

W = 1.5125 GeV

$Q^2 = 0.5\ \mathrm{GeV}^2$

$\Delta Q^2 = 0.2\ \mathrm{GeV}^2$

W = 1.6625 GeV

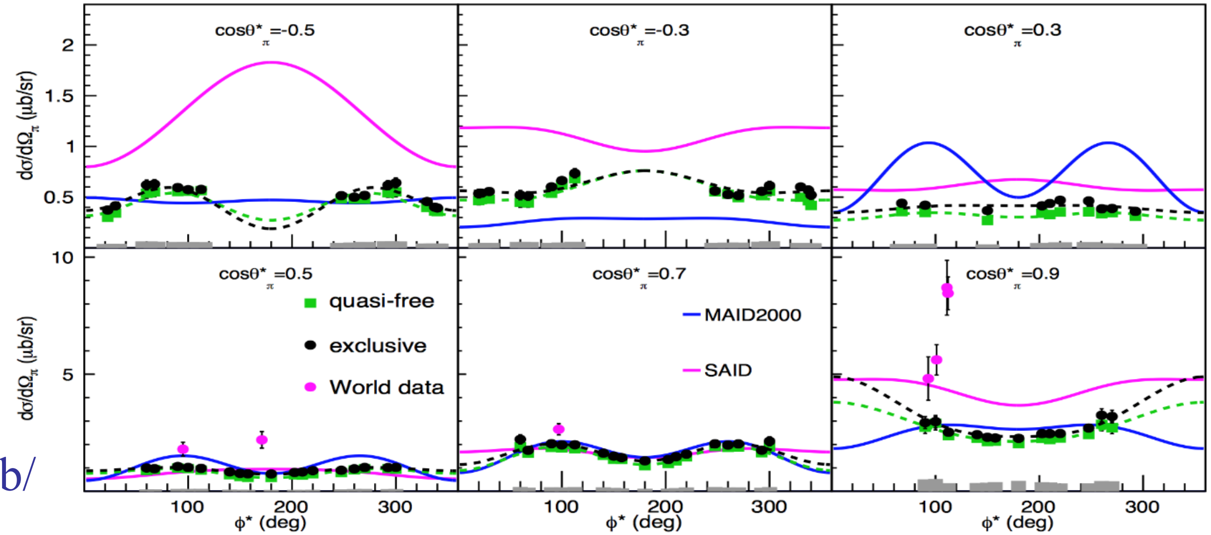

CLAS Database:
https://clasweb.jlab.org/physicsdb/

cos θ_π- Dependent Structure Functions @ W=1.2125 GeV

W = 1.2125 GeV   ΔW = 25 MeV   Ye Tian

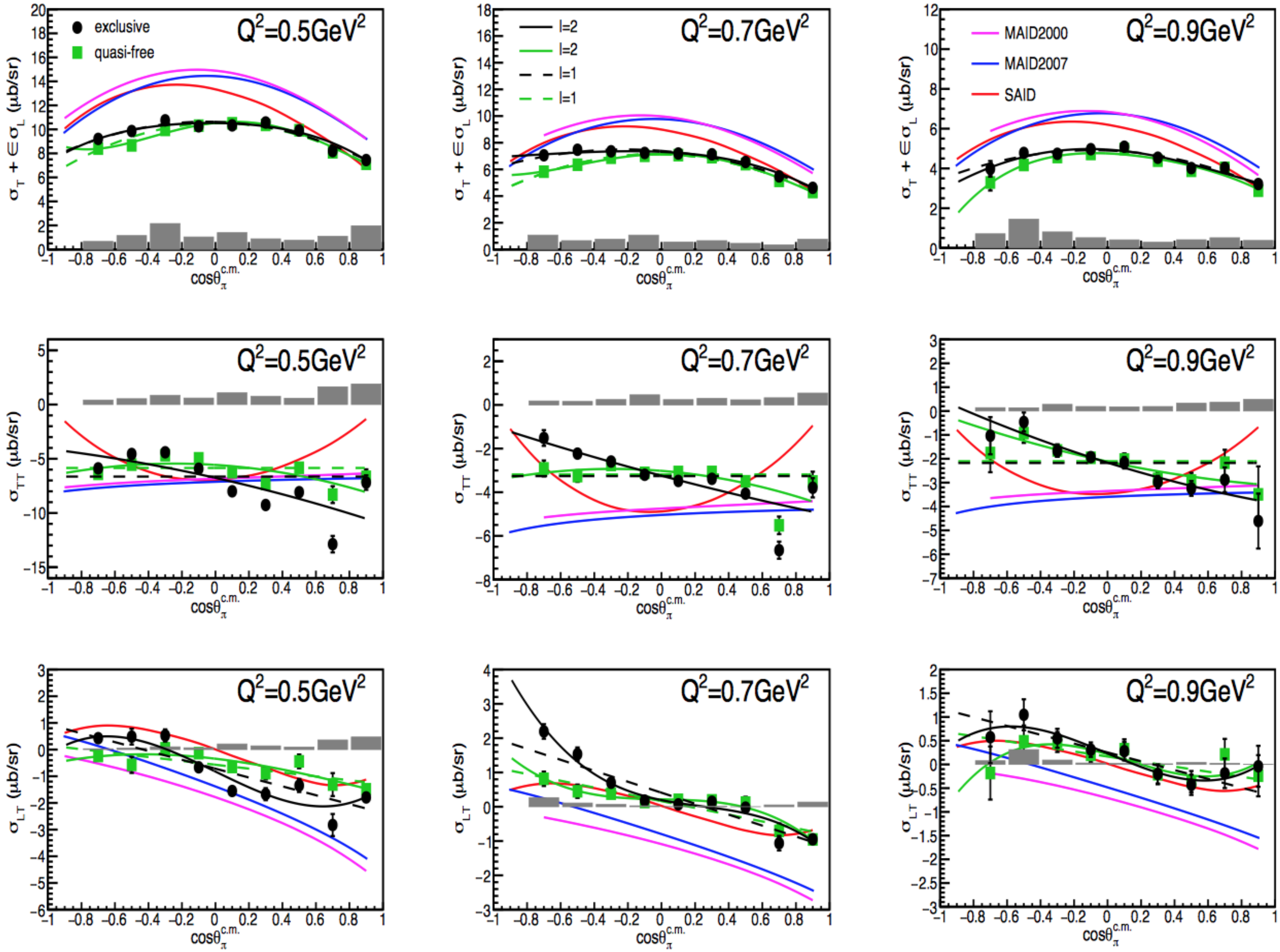

Roper Transition Form Factors in CSM Approach

$N(1440)P_{11}$

J. Segovia *et al.*, Phys. Rev. Lett. 115, 171801 (2015)

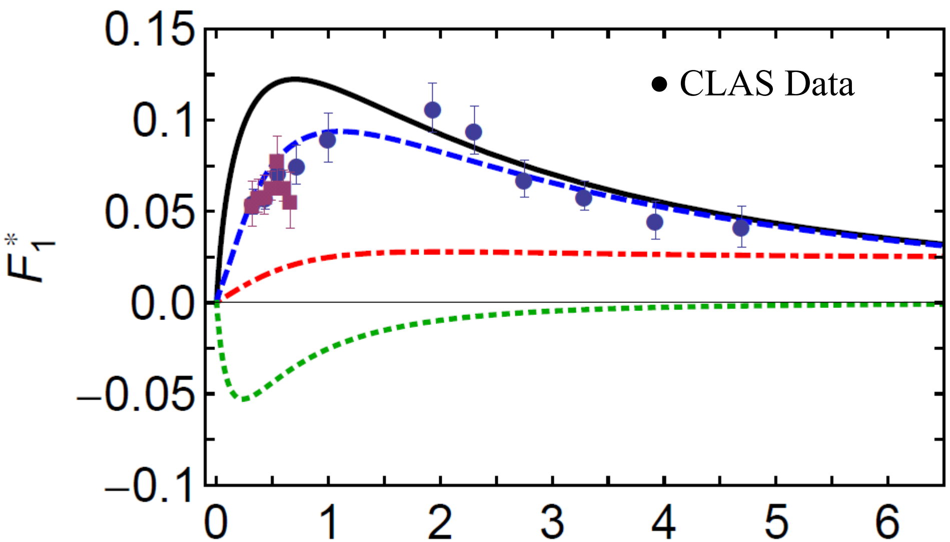

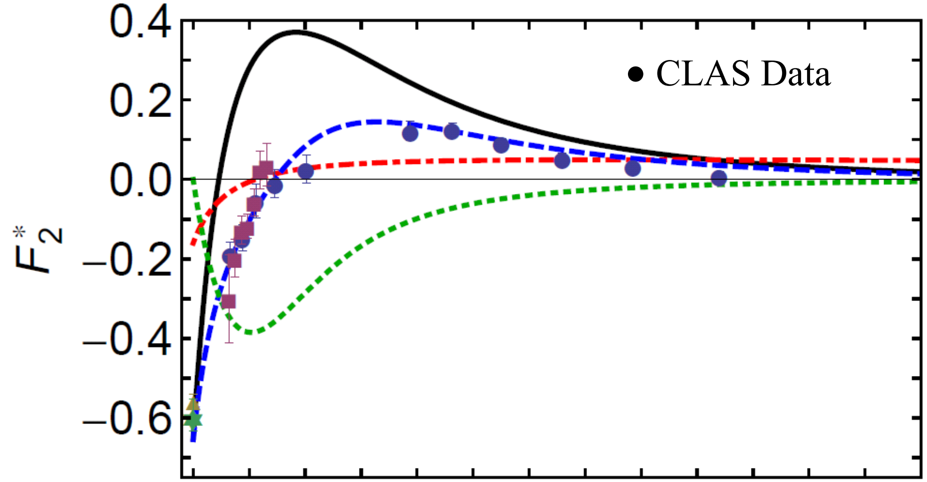

$x = Q^2/m_N^2$

DSE Contact

DSE Realistic

Inferred meson-cloud contribution

Anticipated complete result

Importantly, the existence of a zero in F_2 is not influenced by meson-cloud effects, although its precise location is.

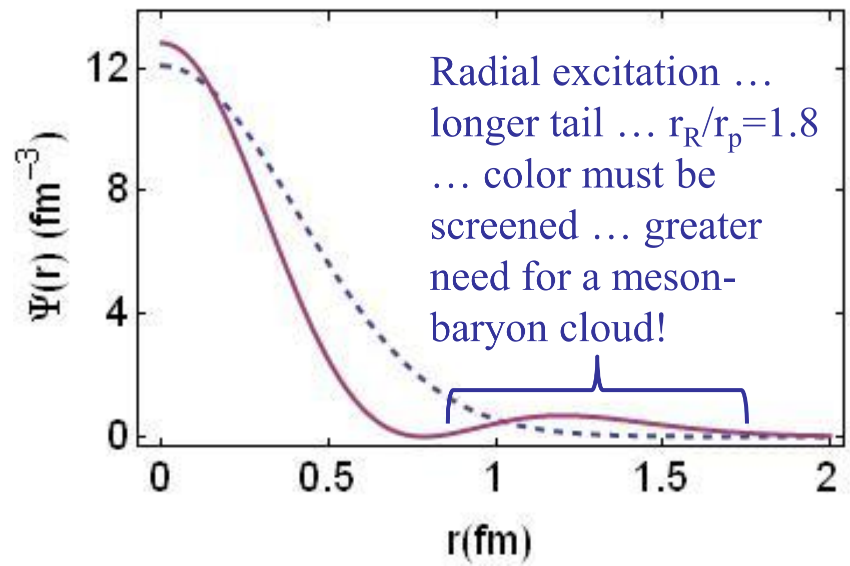

Roper Transition Form Factors in CSM Approach

$N(1440)P_{11}$

Y. Tian *et al.*, Phys. Rev. **C 107**, 015201 (2023) 26

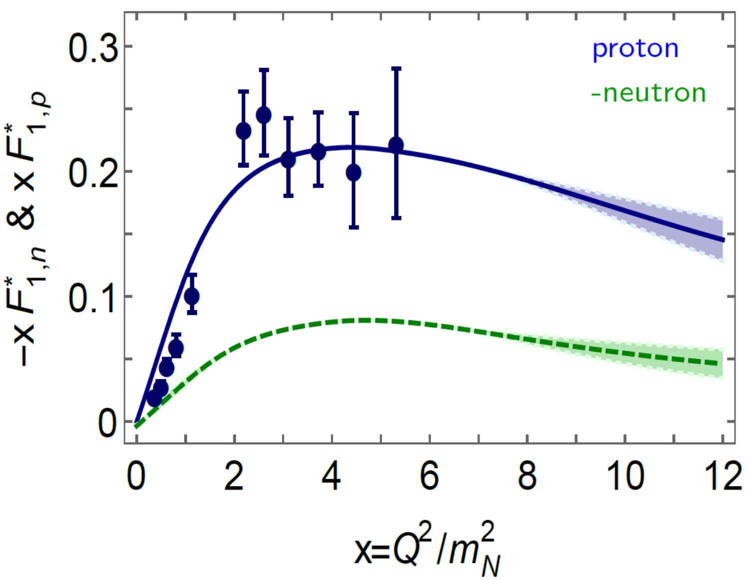

W = 1.2125 GeV

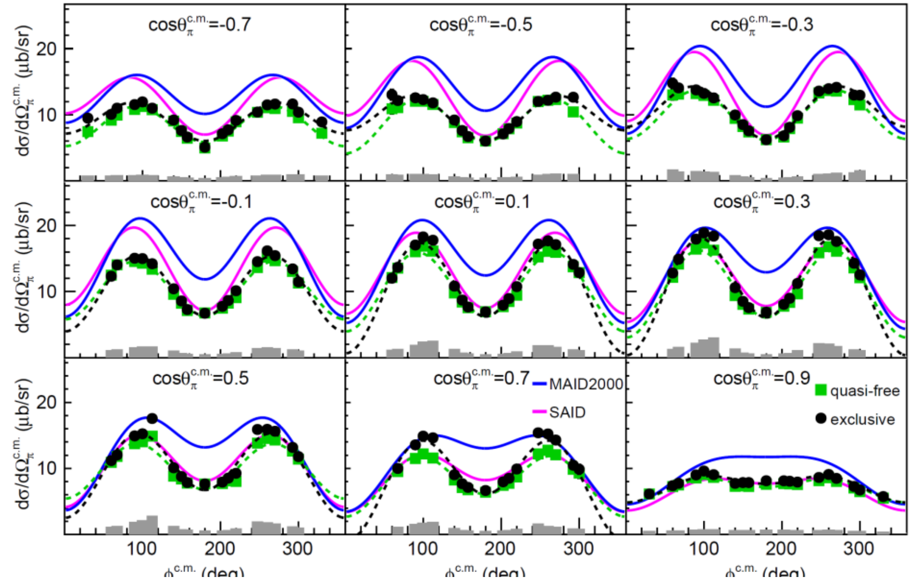

W = 1.5125 GeV

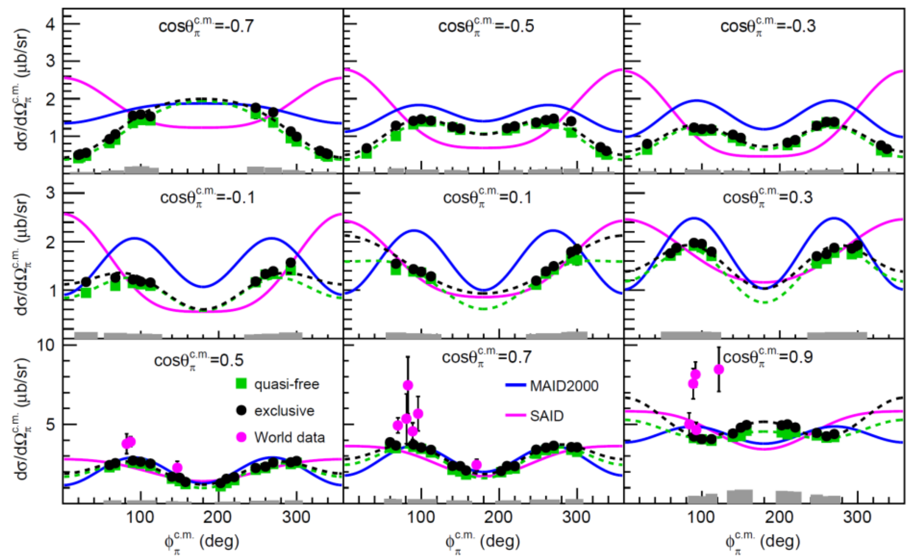

Data-Driven Data Analyses

Consistent Results

Double Pion

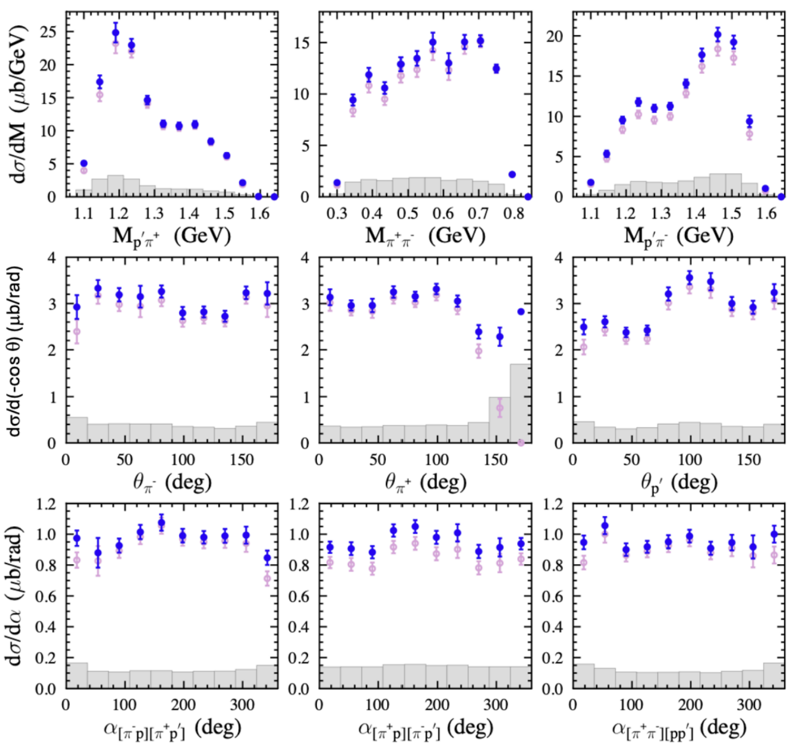

Arjun Trivedi *et al.*, arxiv:2607.06793 (2026)

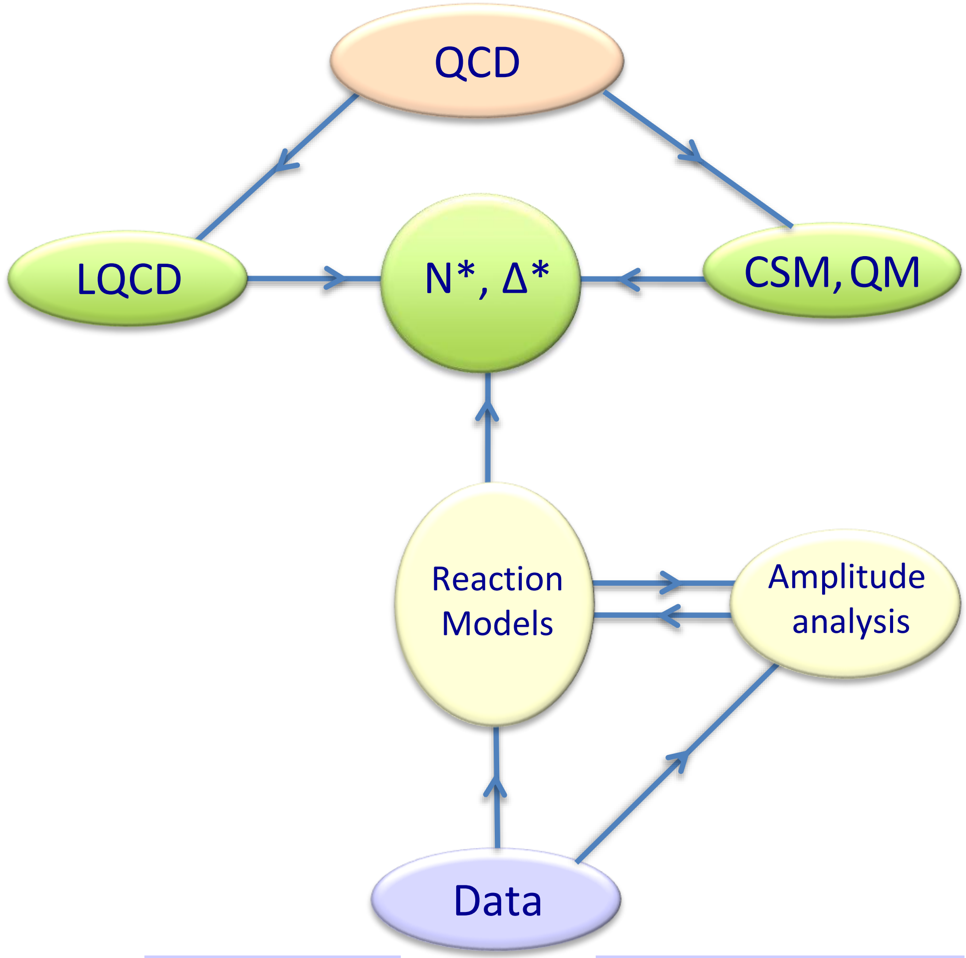

Hadronic production

Electromagnetic production

φ-independent Nππ Single-Differential Cross Sections

$Q^2, W \text{ bin} = [2.4, 3.0) GeV^2, [1.725, 1.750) GeV$

Arjun Trivedi

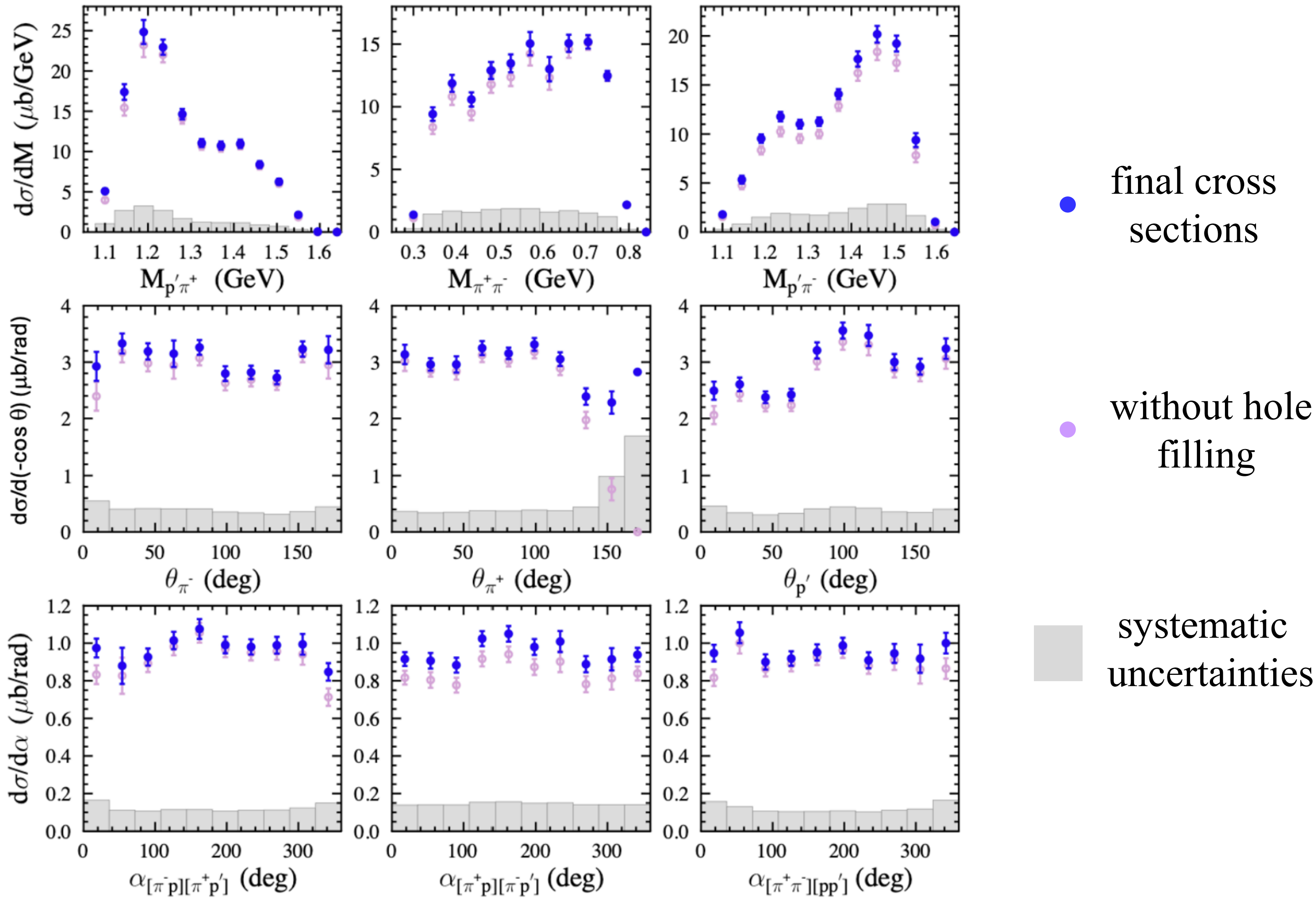

$$\left(\frac{d^2\sigma}{dX_{ij}d\phi_i}\right) = \underline{R2_T{}^{X_{ij}} + R2_L{}^{X_{ij}}} + R2_{LT}{}^{c,X_{ij}}\cos\phi_i + R2_{TT}{}^{c,X_{ij}}\cos 2\phi_i + \delta_{X_{ij}\alpha_i}\left(R2_{LT}{}^{s,\alpha_i}\sin\phi_i + R2_{TT}{}^{s,\alpha_i}\sin 2\phi_i\right)$$

φ-dependent Nππ Single-Differential Cross Sections

Q^2, W bin $= [2.4, 3.0)GeV^2, [1.725, 1.750)GeV$

Arjun Trivedi

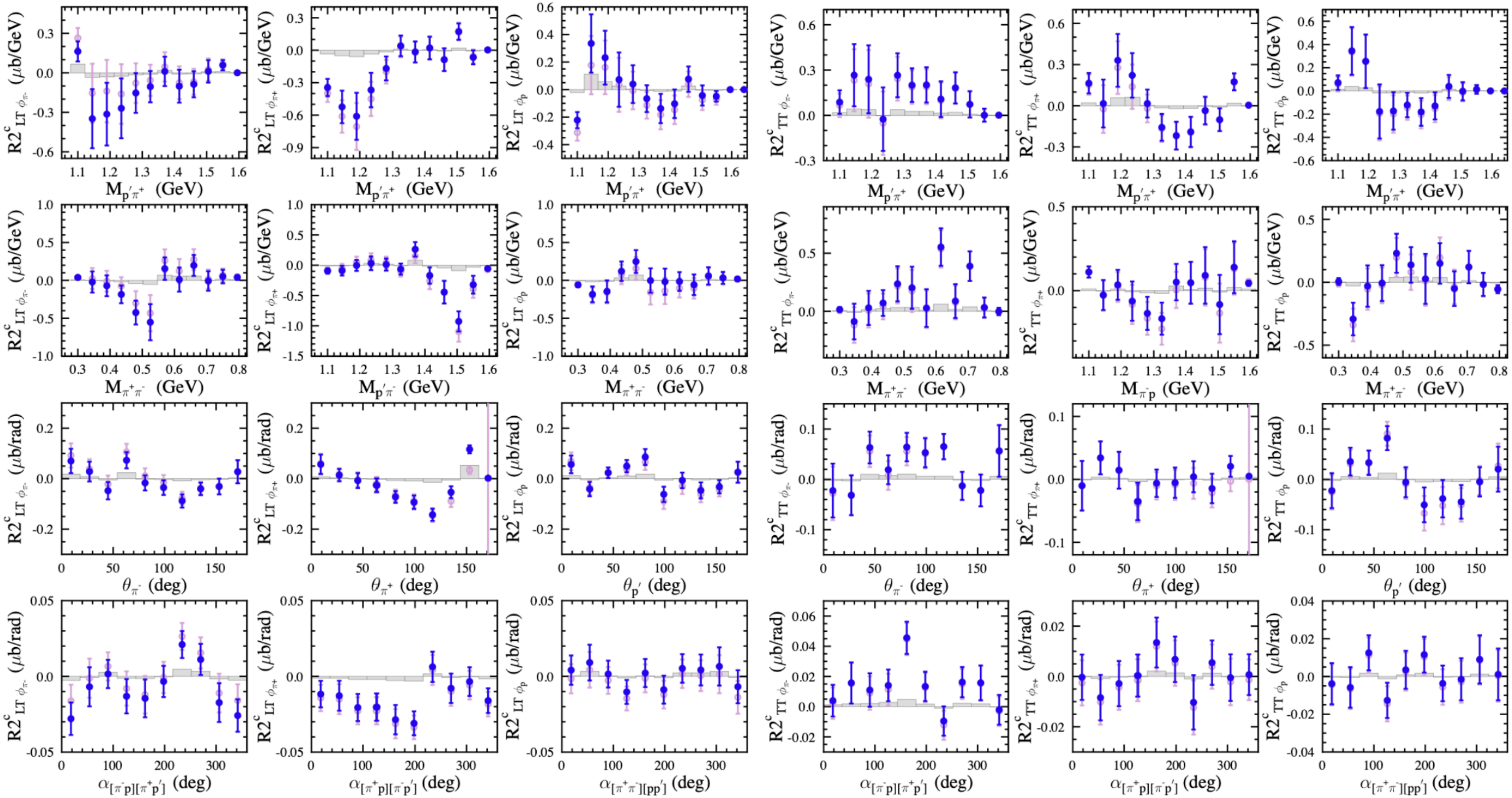

$$\left(\frac{d^2\sigma}{dX_{ij}d\phi_i}\right) = R2_T{}^{X_{ij}} + R2_L{}^{X_{ij}} + \underline{R2_{LT}{}^{c,X_{ij}}\cos\phi_i} + \underline{R2_{TT}{}^{c,X_{ij}}\cos 2\phi_i} + \delta_{X_{ij}\alpha_i}\left(R2_{LT}{}^{s,\alpha_i}\sin\phi_i + R2_{TT}{}^{s,\alpha_i}\sin 2\phi_i\right)$$

φ-dependent Nππ Single-Differential Cross Sections

Arjun Trivedi

$Q^2, W \text{ bin} = [2.4, 3.0) GeV^2, [1.725, 1.750) GeV$

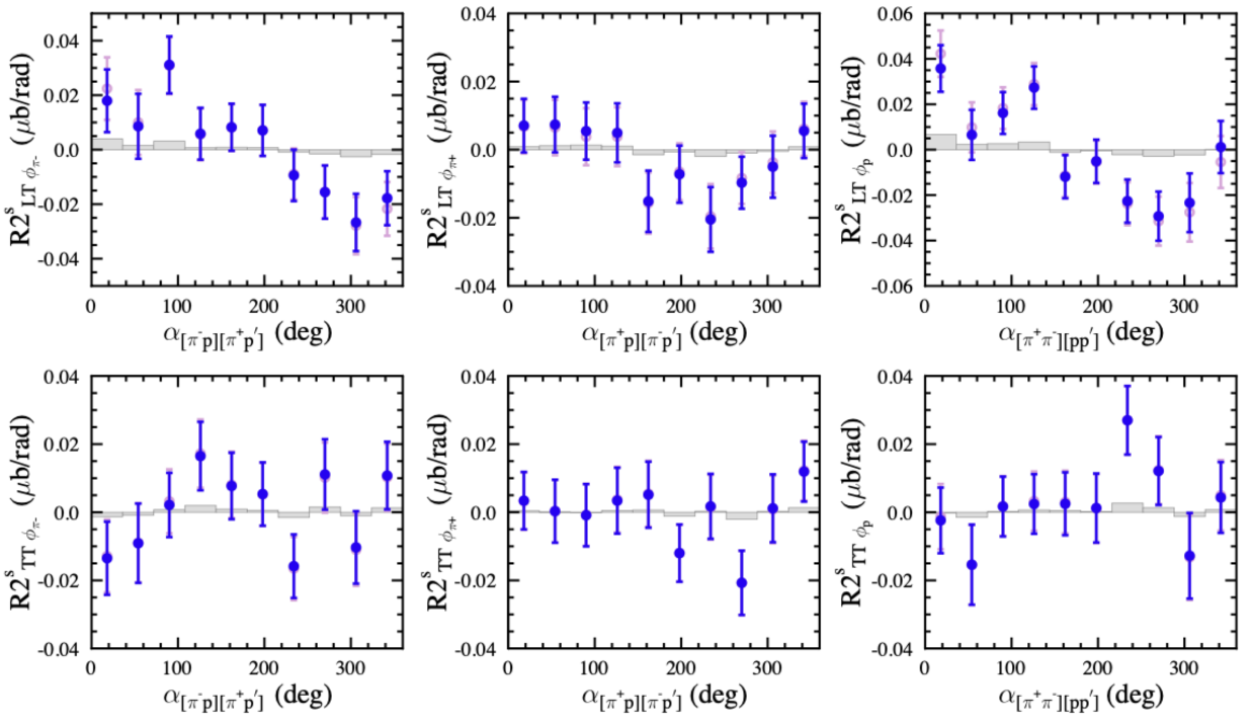

$$\left(\frac{d^2\sigma}{dX_{ij}\,d\phi_i}\right) = R2_T{}^{X_{ij}} + R2_L{}^{X_{ij}} + R2_{LT}{}^{c,X_{ij}}\cos\phi_i + R2_{TT}{}^{c,X_{ij}}\cos 2\phi_i + \delta_{X_{ij}\alpha_i}\left(\underline{R2_{LT}{}^{s,\alpha_i}\sin\phi_i} + \underline{R2_{TT}{}^{s,\alpha_i}\sin 2\phi_i}\right)$$

$N\pi^+\pi^-$ Electroproduction Kinematic Coverage

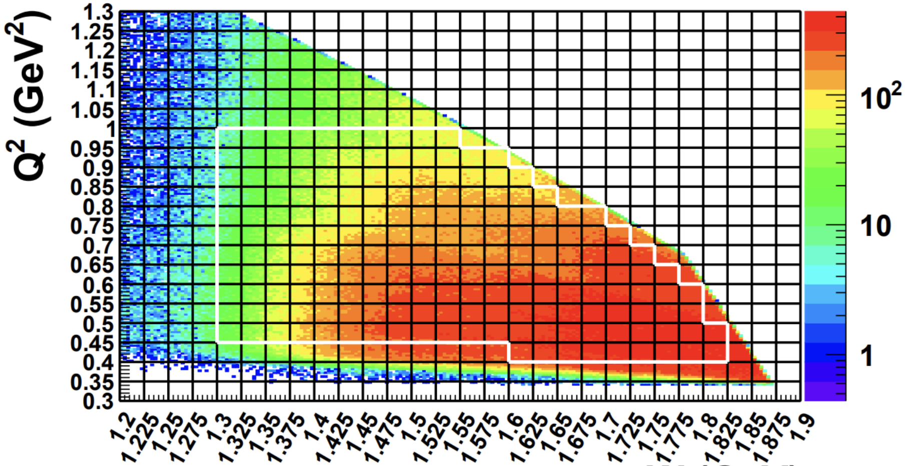

G. Fedotov, I. Sorodumina *et al.*,
Phys. Rev. **C** 98, 025203 (2018)

CLAS12

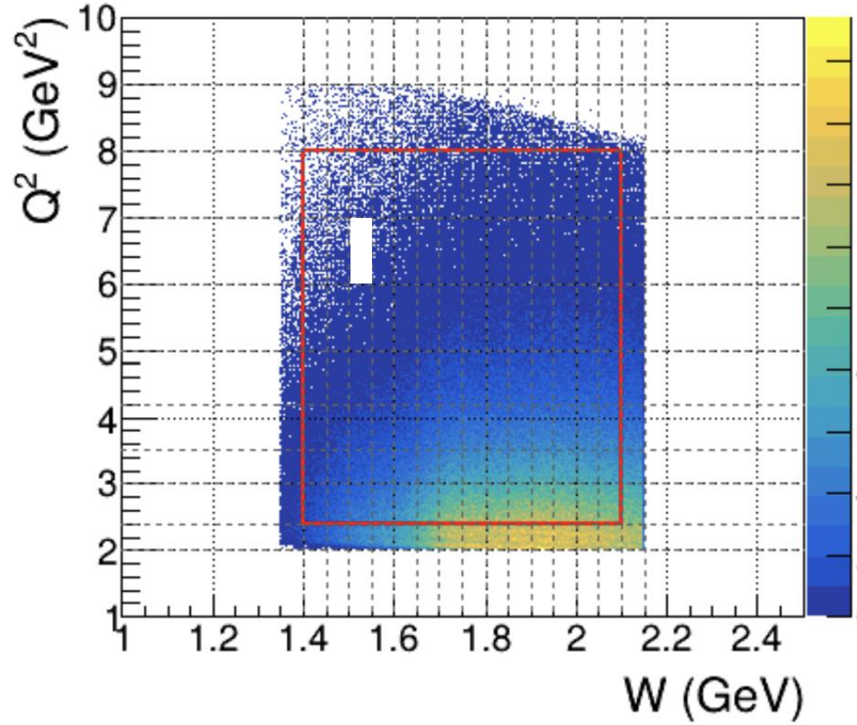

Krishna Neupane et al. (2026)
under CLAS Collaboration Review

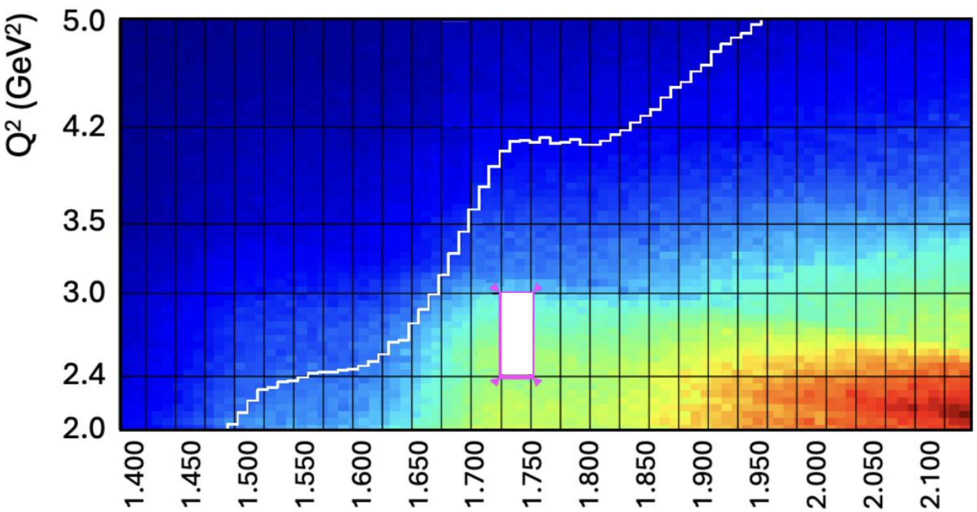

Arjun Trivedi *et al.*, arxiv:2607.06793 (2026)

$N\pi\pi$ Single-Differential Cross Sections

$W \in [1.75, 1.80]$ GeV and $Q^2 \in [3.0, 3.5]$ GeV^2

Krishna Neupane
Arjun Trivedi

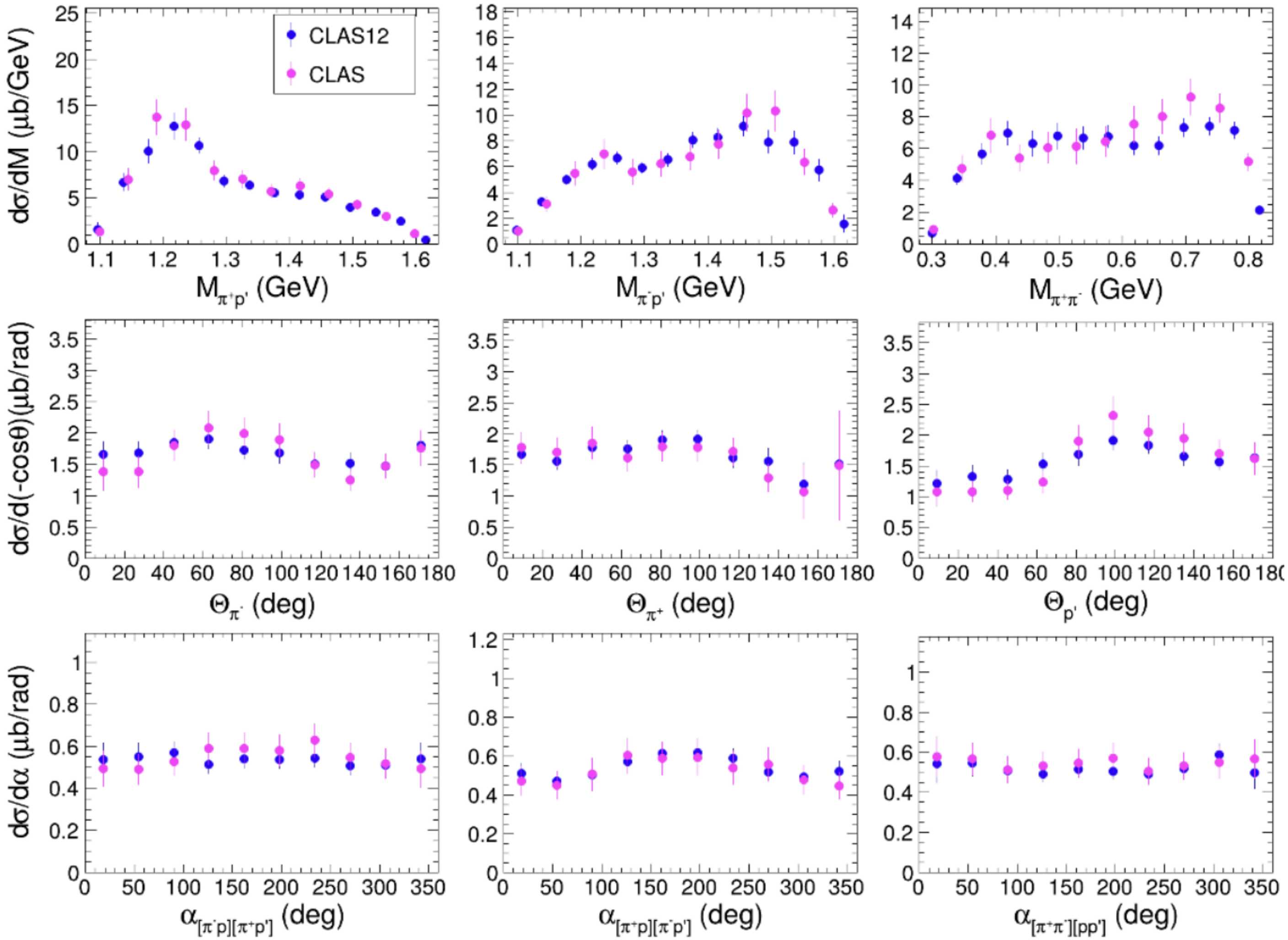

- Krishna
- Arjun

$$\left(\frac{d^2\sigma}{dX_{ij}\,d\phi_i}\right) = \underline{R2_T{}^{X_{ij}} + R2_L{}^{X_{ij}}} + R2_{LT}{}^{c,X_{ij}}\cos\phi_i + R2_{TT}{}^{c,X_{ij}}\cos 2\phi_i + \delta_{X_{ij}\alpha_i}\left(R2_{LT}{}^{s,\alpha_i}\sin\phi_i + R2_{TT}{}^{s,\alpha_i}\sin 2\phi_i\right)$$

Nππ Single-Differential Cross Sections

W ∈ [1.50, 1.55] GeV and Q^2 ∈ [6.0, 7.0] GeV^2

Krishna Neupane

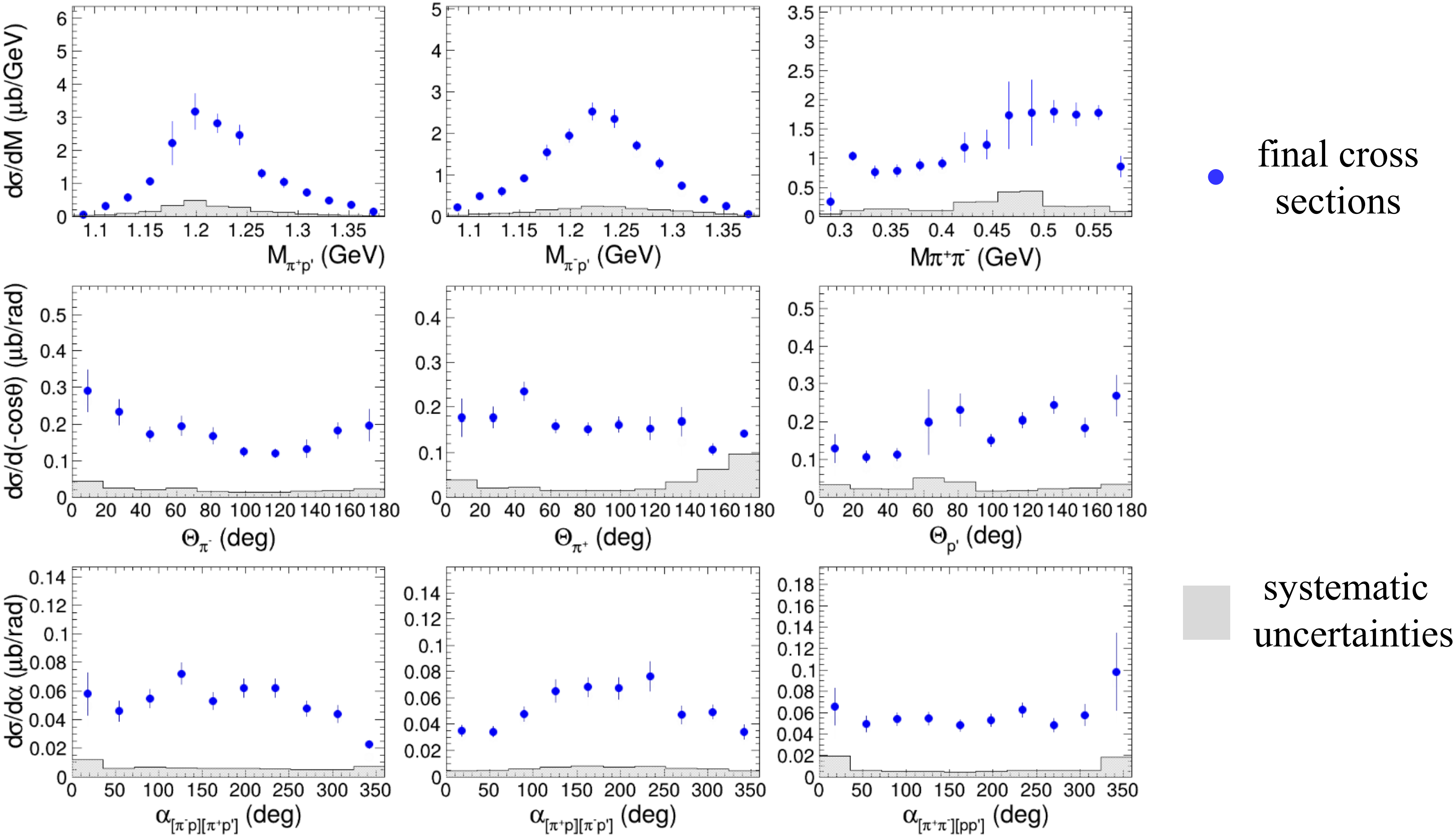

$$\left(\frac{d^2\sigma}{dX_{ij}\,d\phi_i}\right) = \underline{R2_T{}^{X_{ij}} + R2_L{}^{X_{ij}}} + R2_{LT}{}^{c,X_{ij}}\cos\phi_i + R2_{TT}{}^{c,X_{ij}}\cos 2\phi_i + \delta_{X_{ij}\alpha_i}\left(R2_{LT}{}^{s,\alpha_i}\sin\phi_i + R2_{TT}{}^{s,\alpha_i}\sin 2\phi_i\right)$$

Nucleon Resonances in Nπ and Nππ Electroproduction

- Nππ channel is sensitive to N*s heavier than 1.4 GeV
- Provides information that is complementary to the Nπ channel
- Many higher-lying N*s decay preferentially into Nππ final states

1) Bianca Gualtieri: KY

4) Zhaozhong Shi: ω(782)

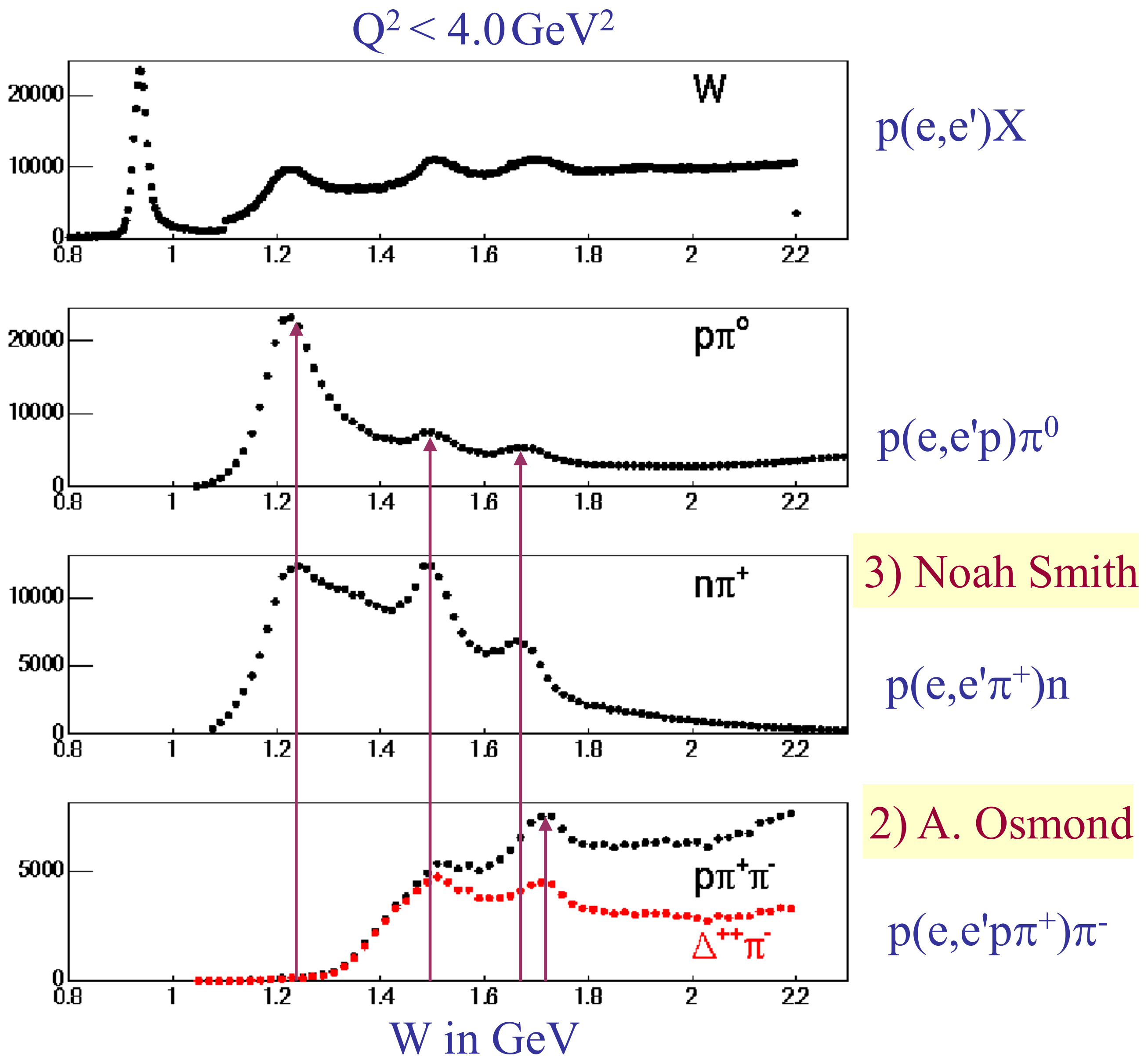

Phenomenological Analysis

Data-Driven Data Analyses

Consistent Results

- Single meson production:
  Unitary Isobar Model (JANR, MAID, SAID)
  Fixed-*t* Dispersion Relations (JANR)
- Double pion production:
  Unitarized Isobar Model (JM)
- Coupled-Channel Approaches: 5) Ahmed M. Foda
  EBAC ⇒ Argonne-Osaka
  JBW ⇒ Jülich-Bonn-Washington
  BoGa ⇒ Bonn-Gatchina

M. Mai, M. Döring tomorrow

Int. J. Mod. Phys. E, Vol. 22, 1330015 (2013) 1-99

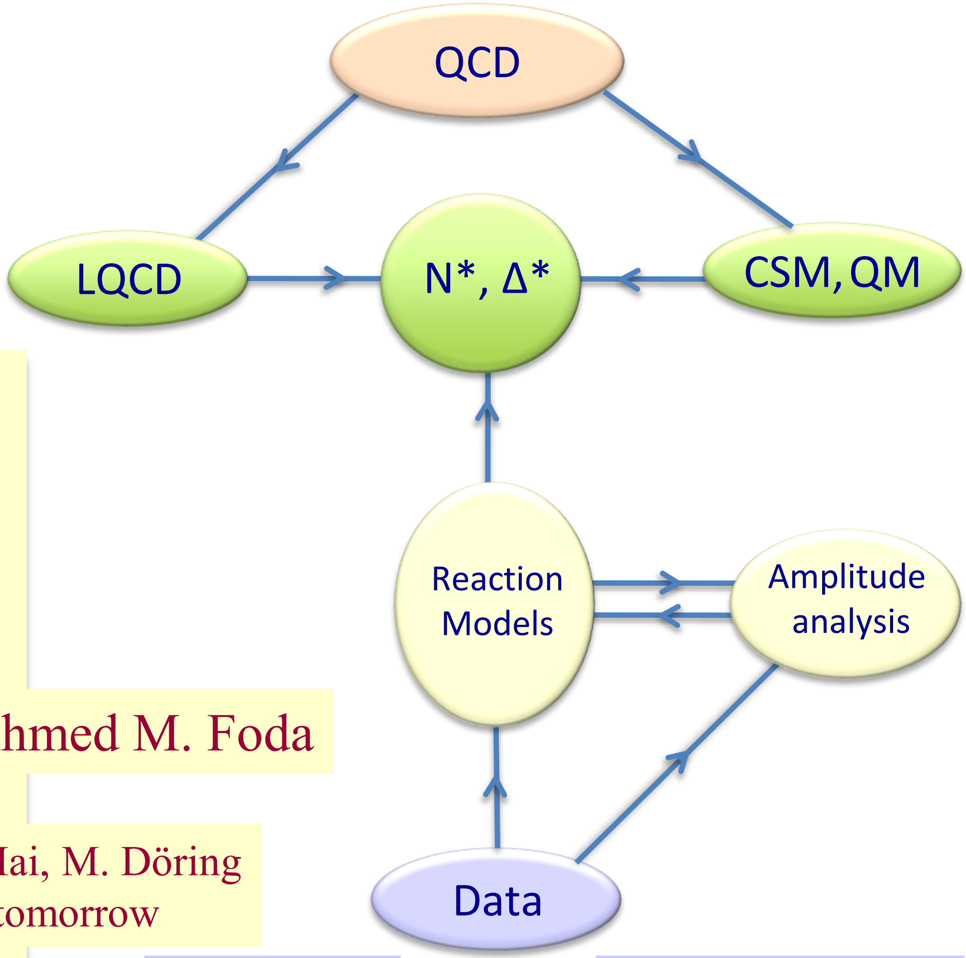

Hadronic production

Electromagnetic production

N(1440)1/2$^+$ Couplings from CLAS

Viktor Mokeev

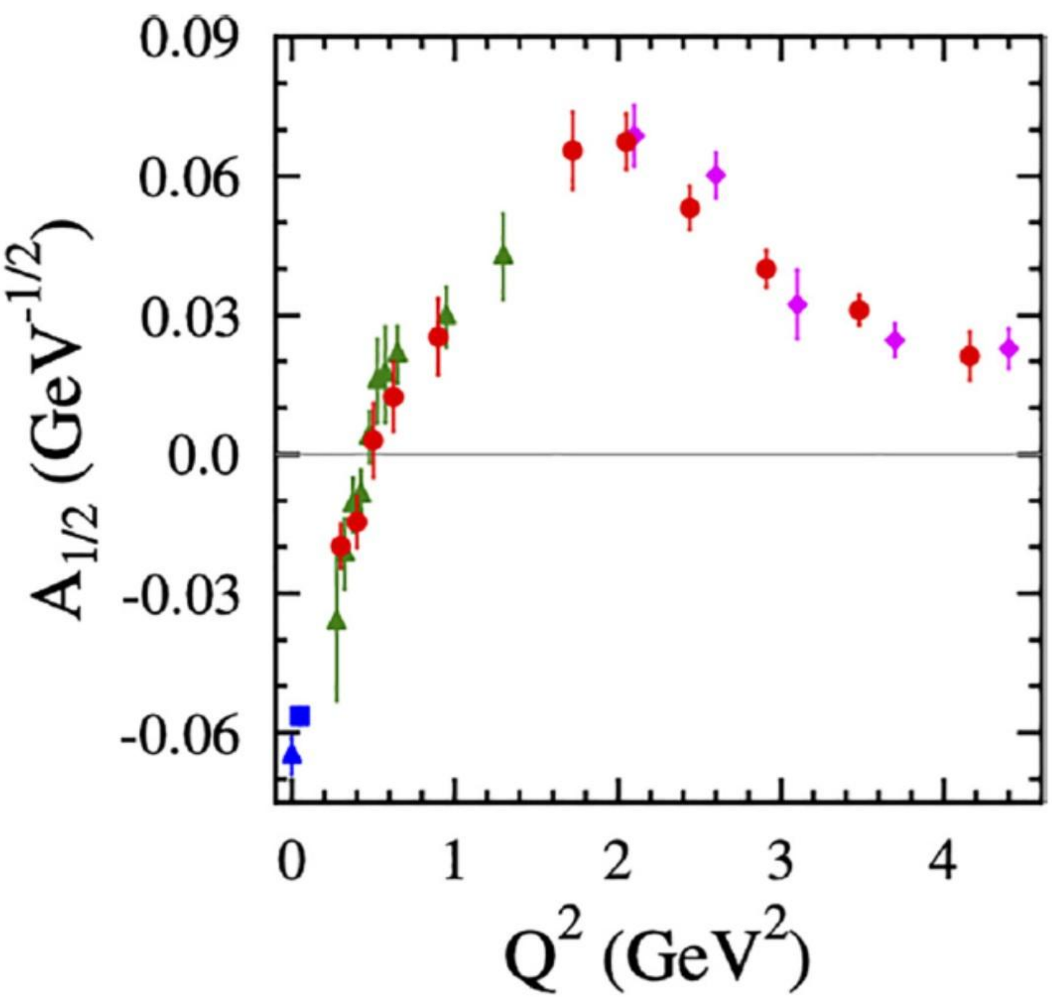

Consistent results are now obtained in the low-lying resonance region up to a Q^2 of 5 GeV^2 by independent analyses from the $N\pi$ differential cross sections, beam, target, and beam-target asymmetries (red bullets, left) and $p\pi^+\pi^-$ differential cross sections (purple diamonds, green triangles). All observables have fundamentally different mechanisms for the nonresonant background and underscore the capability of the reaction models to extract reliable resonance electrocouplings.

V. Mokeev *et al.*, Phys. Rev. C 108, 025204 (2023) 1-26

N(1440)1/2$^+$ Couplings from CLAS

Viktor Mokeev

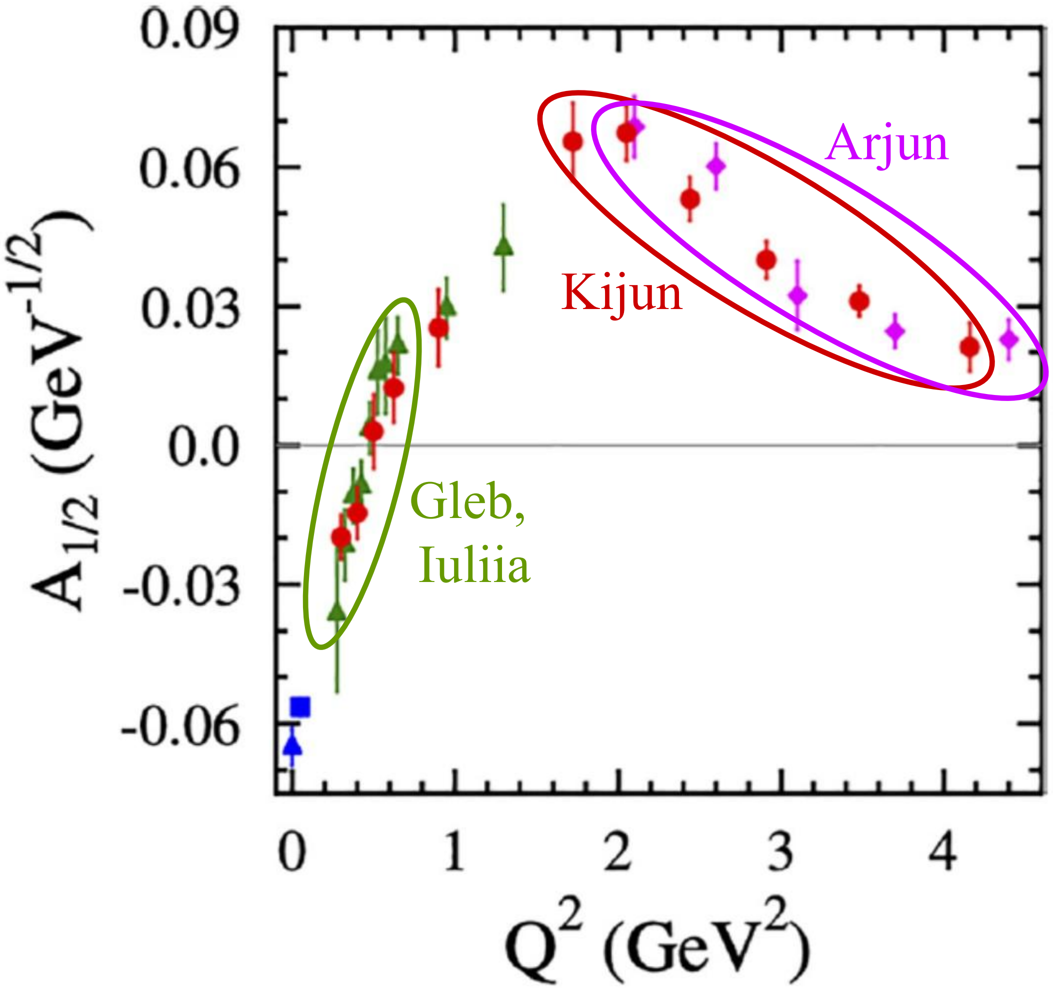

Consistent results are now obtained in the low-lying resonance region up to a Q^2 of 5 GeV^2 by independent analyses from the $N\pi$ differential cross sections, beam, target, and beam-target asymmetries (red bullets, left) and $p\pi^+\pi^-$ differential cross sections (purple diamonds, green triangles). All observables have fundamentally different mechanisms for the nonresonant background and underscore the capability of the reaction models to extract reliable resonance electrocouplings.

V. Mokeev *et al*., Phys. Rev. C 108, 025204 (2023) 1-26

N(1440)1/2^{+} Couplings from CLAS

Viktor Mokeev

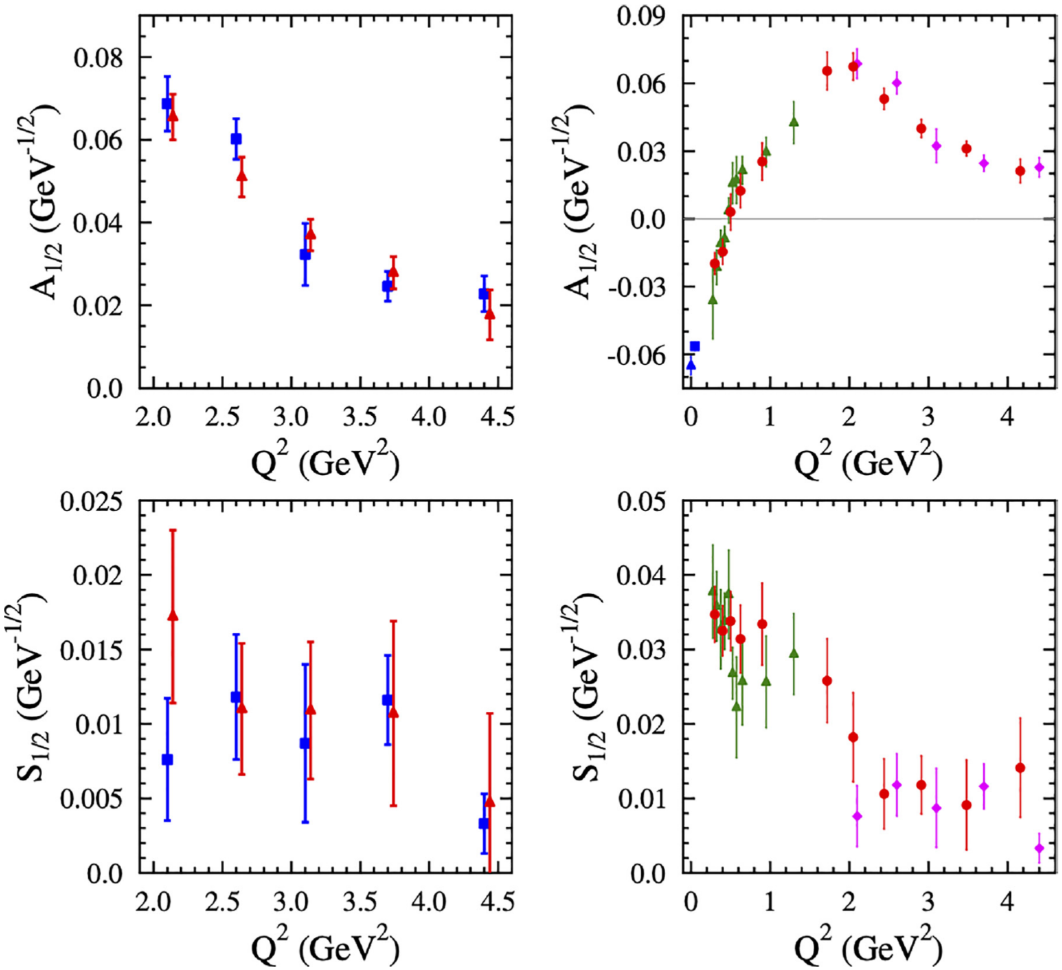

Consistent results are now obtained in the low-lying resonance region up to a Q^2 of 5 GeV^2 by independent analyses from the $N\pi$ differential cross sections, beam, target, and beam-target asymmetries (red triangles, left) and $p\pi^+\pi^-$ differential cross sections (blue squares, left).

All observables have fundamentally different mechanisms for the nonresonant background and underscore the capability of the reaction models to extract reliable resonance electrocouplings.

V. Mokeev *et al.*, Phys. Rev. C 108, 025204 (2023) 1-26

N(1440)1/2$^+$ Couplings from CLAS

Viktor Mokeev

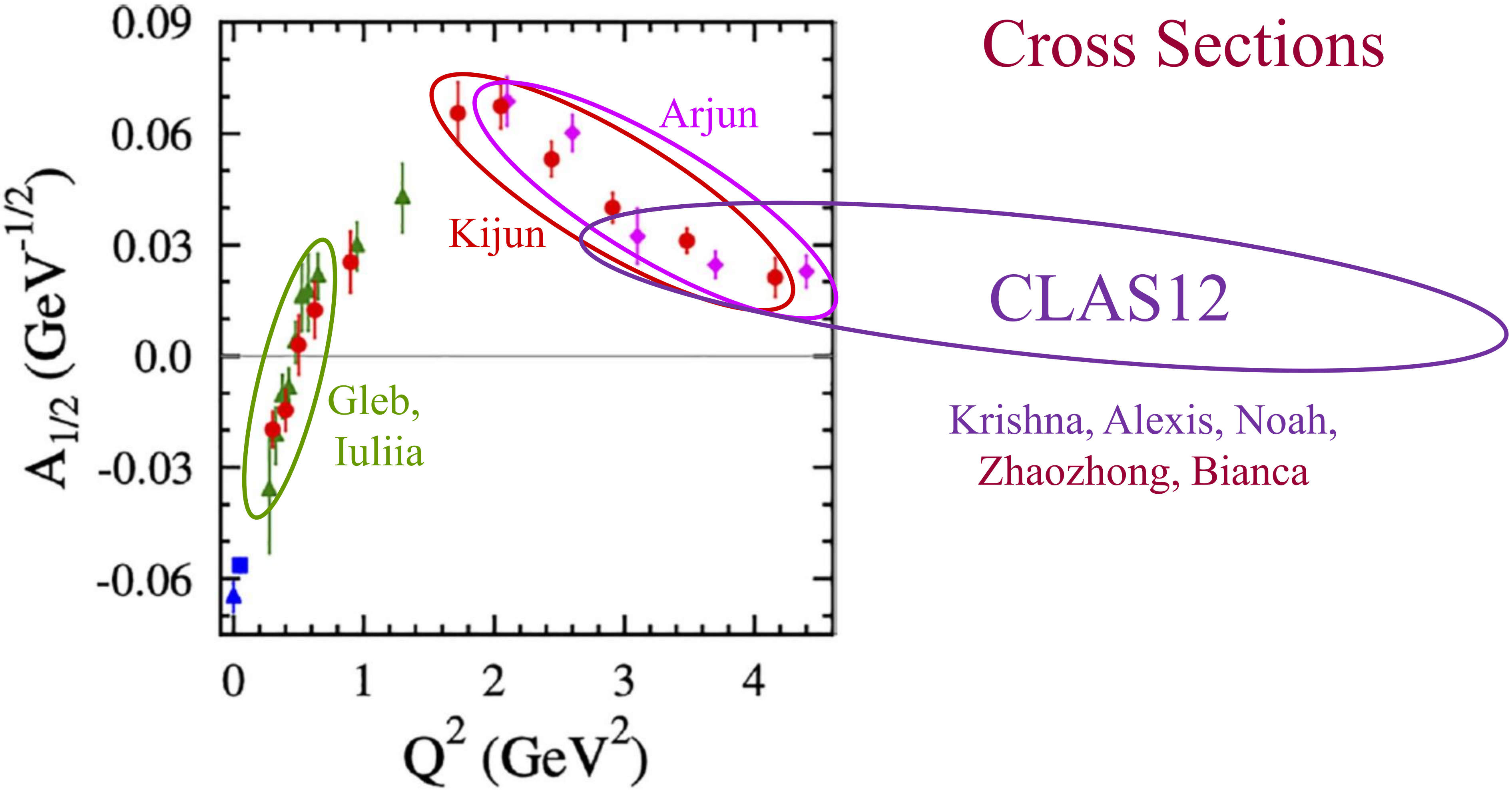

Cross Sections

Krishna, Alexis, Noah,

Zhaozhong, Bianca

V. Mokeev *et al.*, Phys. Rev. C 108, 025204 (2023) 1-26

N(1440)1/2⁺ Couplings from CLAS

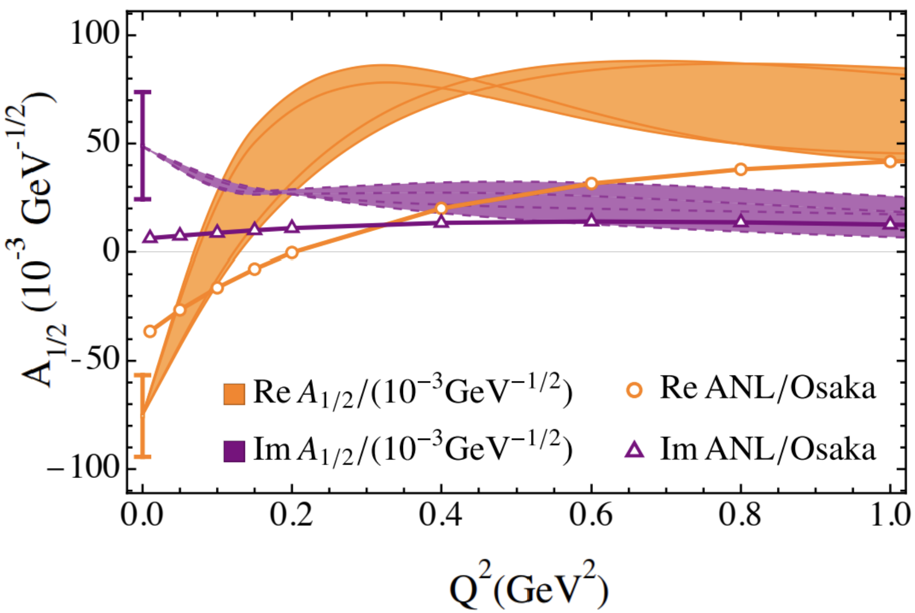

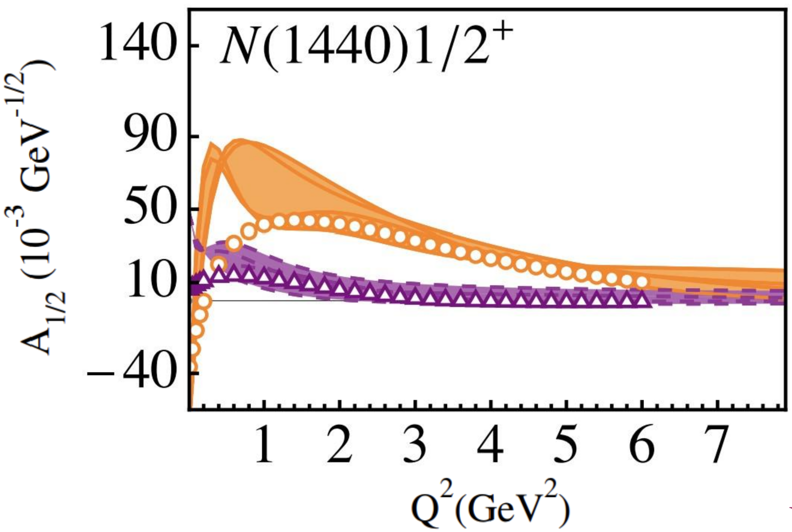

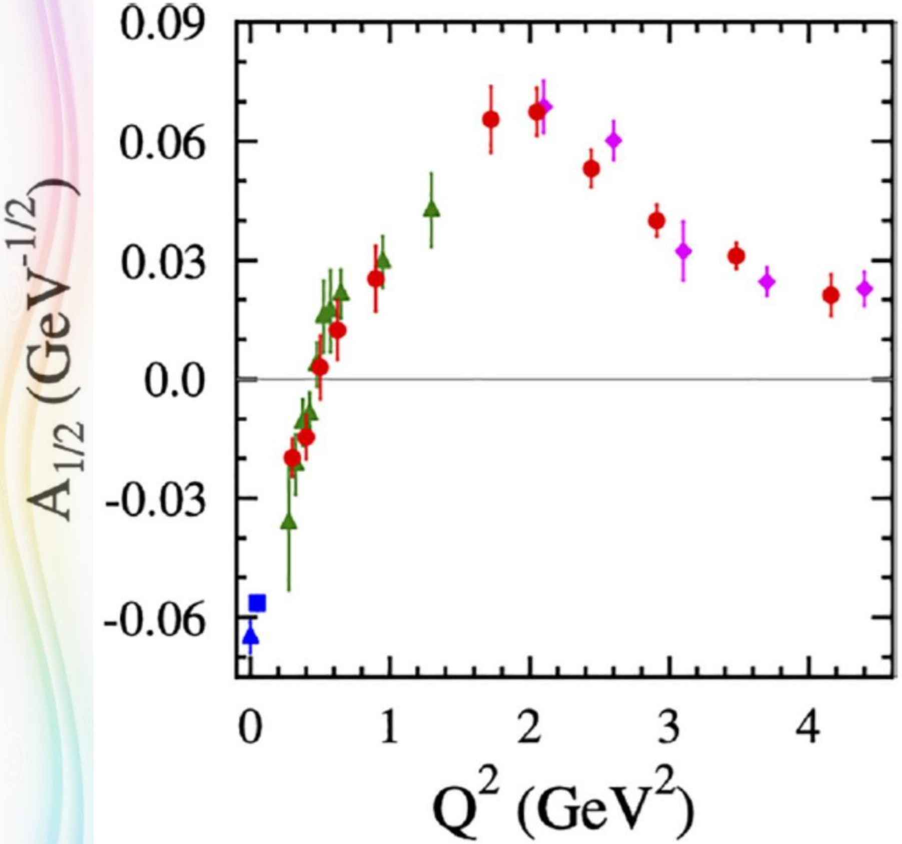

Y.-F. Wang *et al.*, Phys. Rev. Lett. 133, 101901 (2024)

N(1520) $3/2^-$ Couplings from CLAS

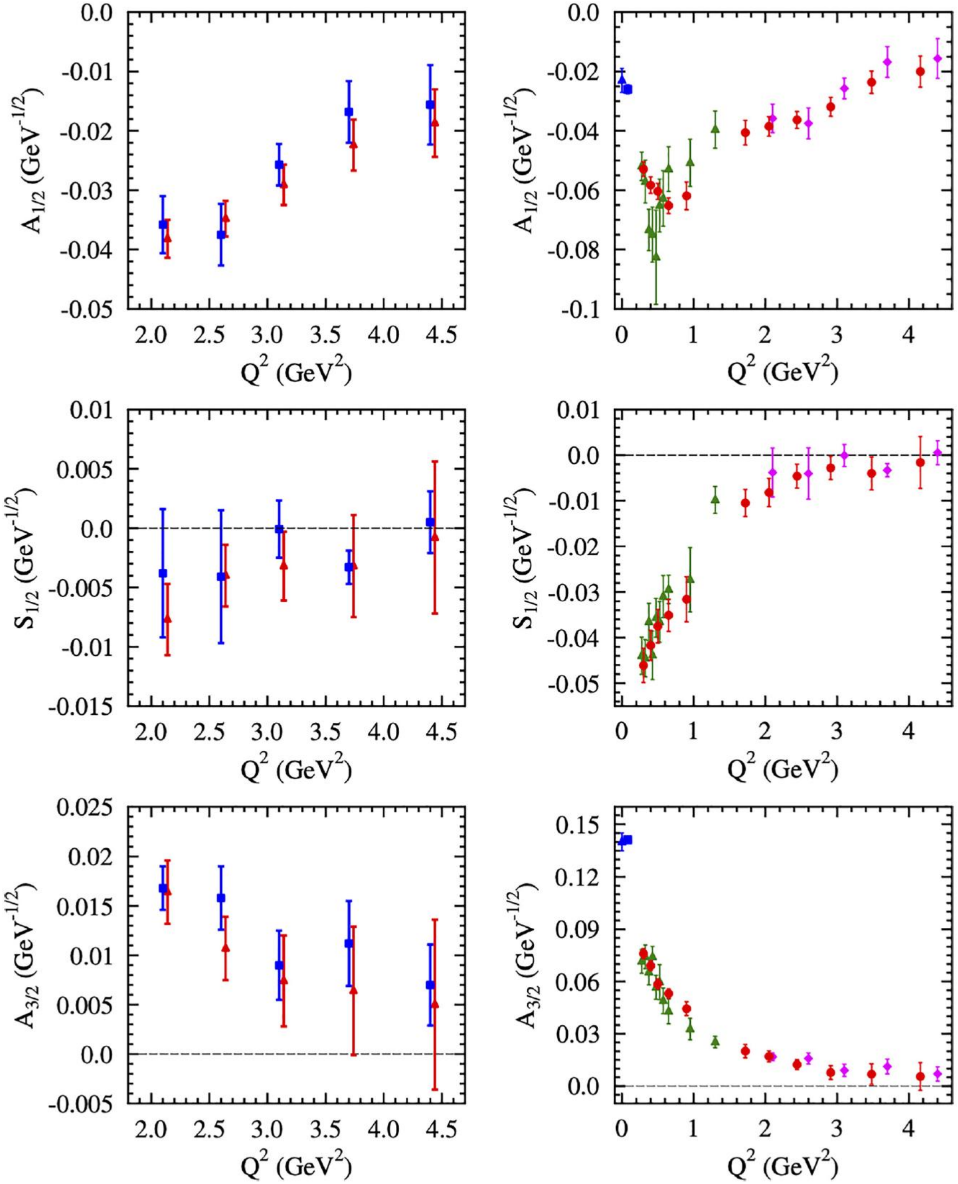

Viktor Mokeev

Consistent results are now obtained in the low-lying resonance region up to a Q^2 of 5 GeV^2 by independent analyses from the $N\pi$ differential cross sections, beam, target, and beam-target asymmetries (red triangles, left) and $p\pi^+\pi^-$ differential cross sections (blue squares, left). All observables have fundamentally different mechanisms for the nonresonant background and underscore the capability of the reaction models to extract reliable resonance electrocouplings.

Phys. Rev. C 108, 025204 (2023) 1-26

$\Delta(1600)3/2^+$ Form Factors in CSM Approach

CSM predictions of the $\Delta(1600)3/2^+$ electrocouplings

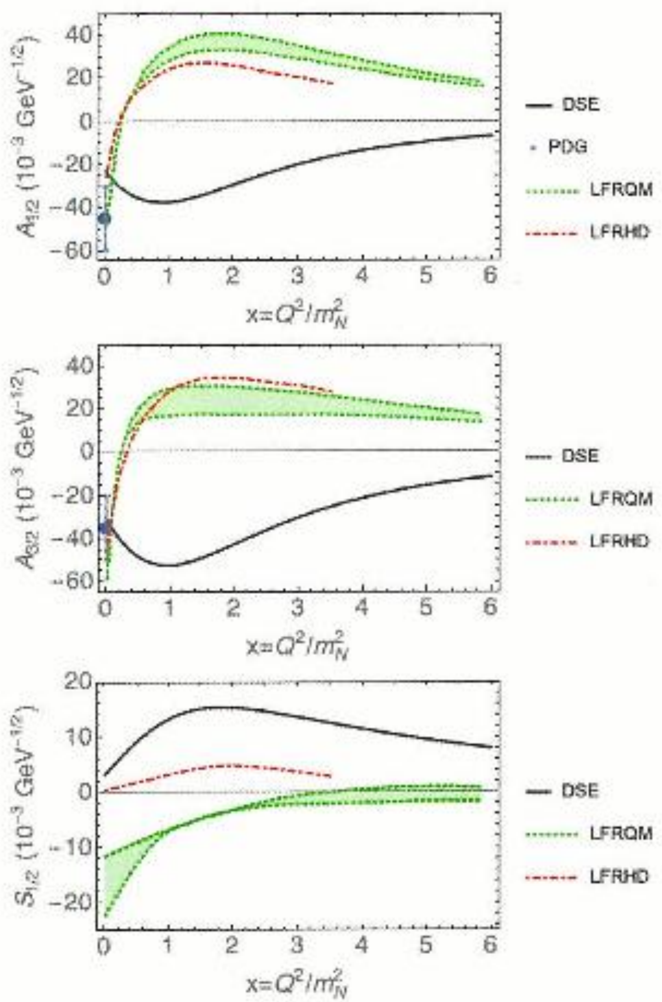

Ya Lu et al., PRD 100, 034001 (2019)

Arjun Trivedi
Viktor Mokeev

W=1.56 GeV, Q^2=2.1 GeV^2

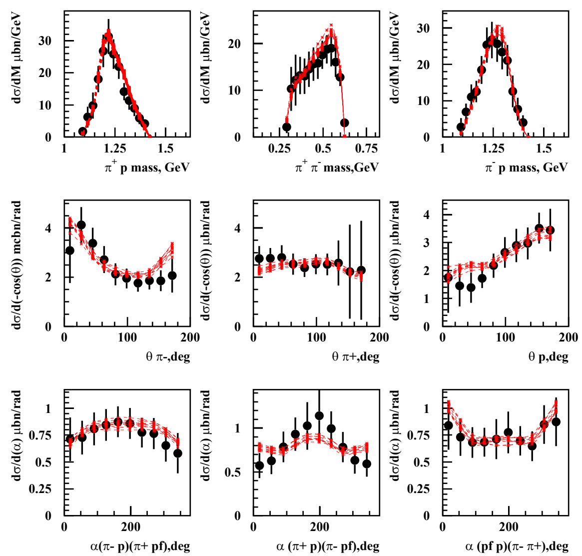

W=1.56 GeV, Q^2=3.1 GeV^2

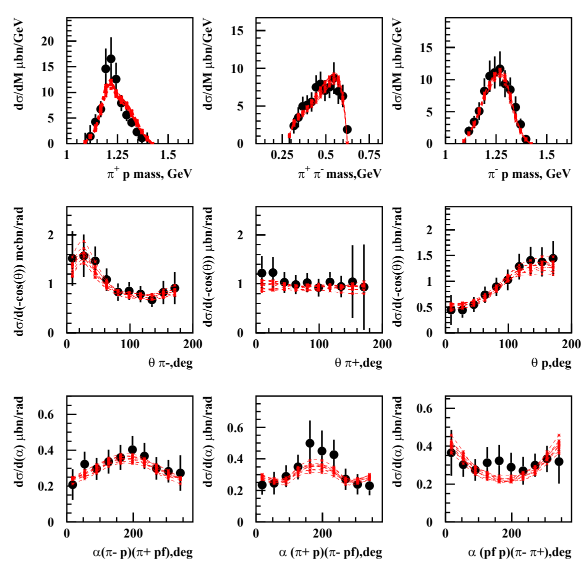

$\Delta(1600)3/2^+$ Form Factors in CSM Approach

Viktor Mokeev

CSM predictions of the $\Delta(1600)3/2^+$ electrocouplings

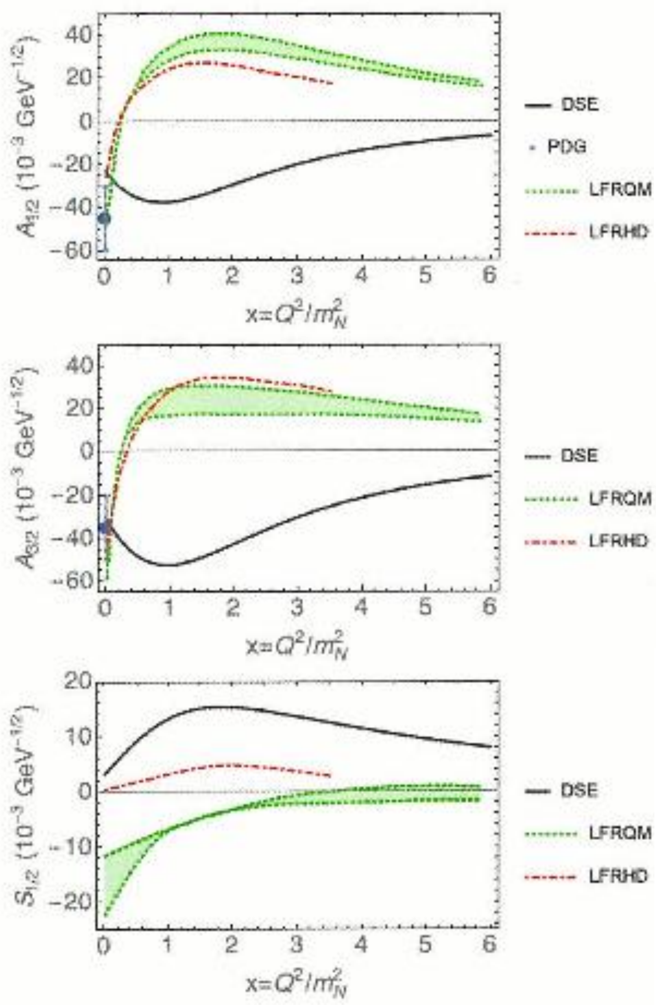

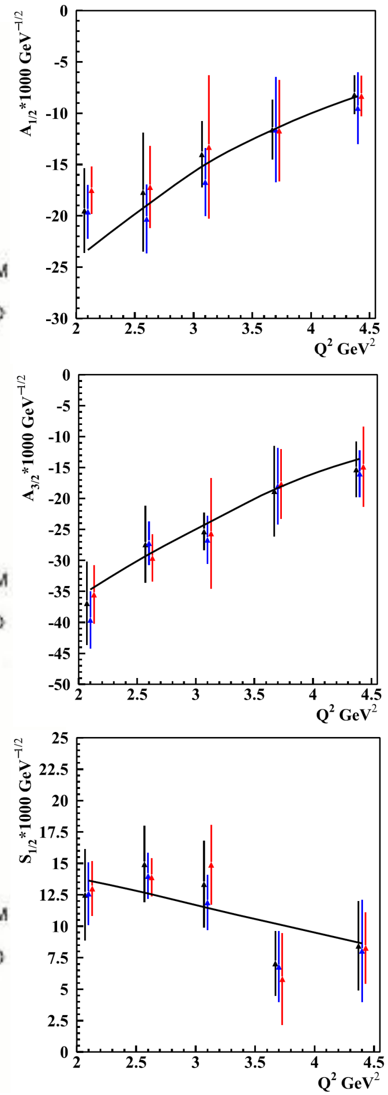

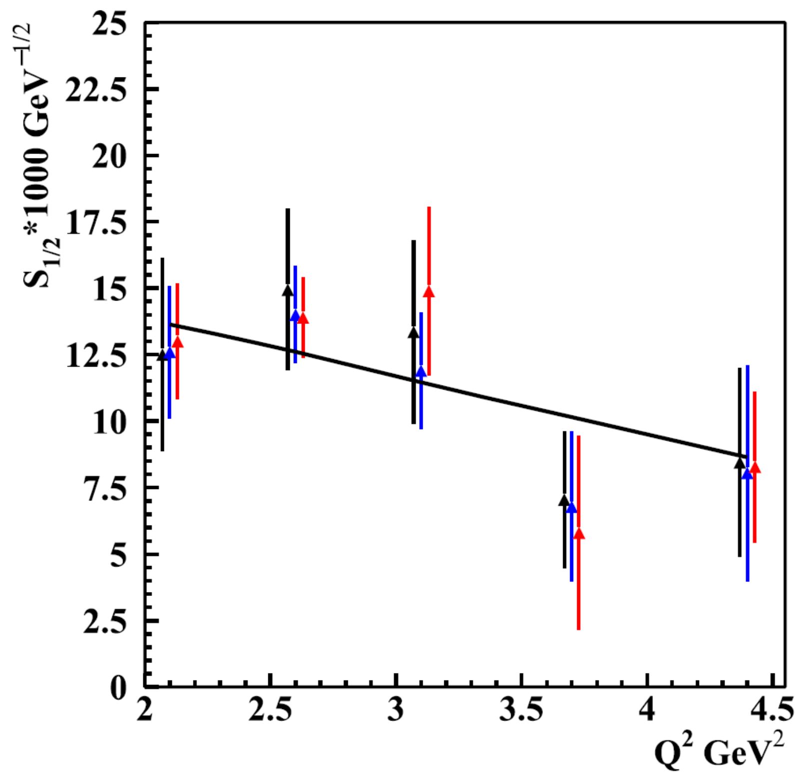

JM analysis of Arjun's $\pi^+\pi^-p$ differential cross sections for $2.0\text{GeV}^2<Q^2<5.0\text{GeV}^2$ within $1.56\text{GeV}<W<1.66\text{GeV}$ and $1.61\text{GeV}<W<1.71\text{GeV}$ with varied compared to previously fixed hadronic parameter for $M_{N*}>1.65$.

Ya Lu et al., PRD 100, 034001 (2019)

Phys. Rev. C 108, 025204 (2023) 1-26

N(1675)5/2$^-$ Couplings from CLAS

Viktor Mokeev

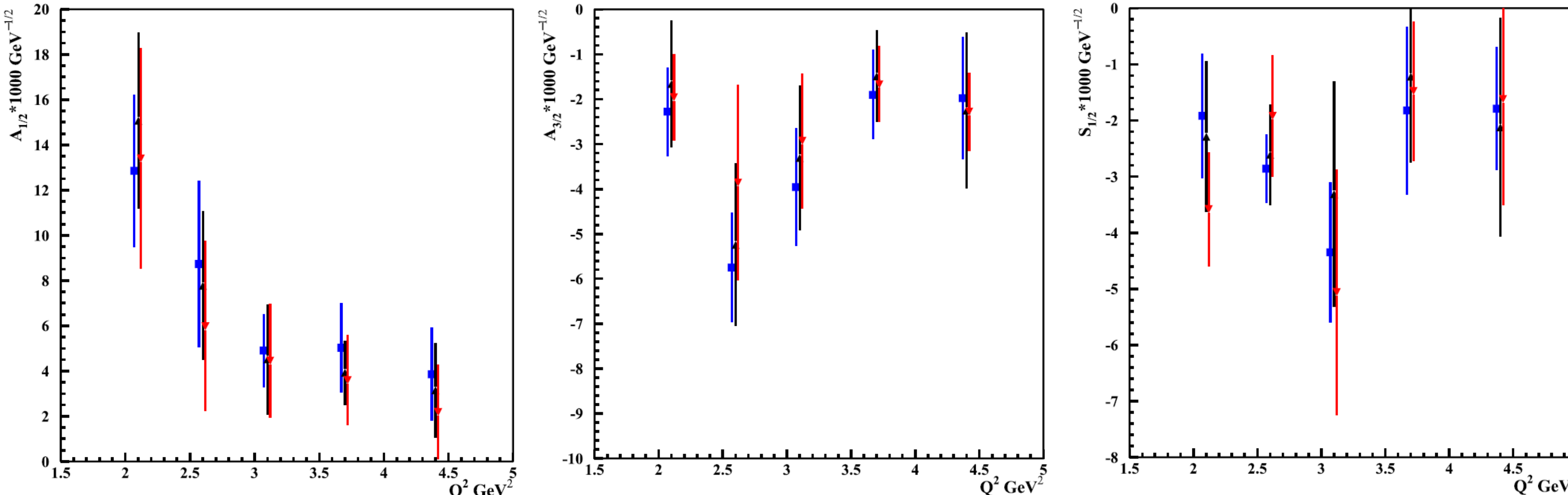

JM23 analysis of Arjun's $\pi^+\pi^-p$ differential cross sections for 2.0GeV^2<Q^2<5.0GeV^2 within 1.56GeV<W<1.66GeV, 1.61GeV<W<1.71GeV, and 1.66GeV<W<1.76GeV.

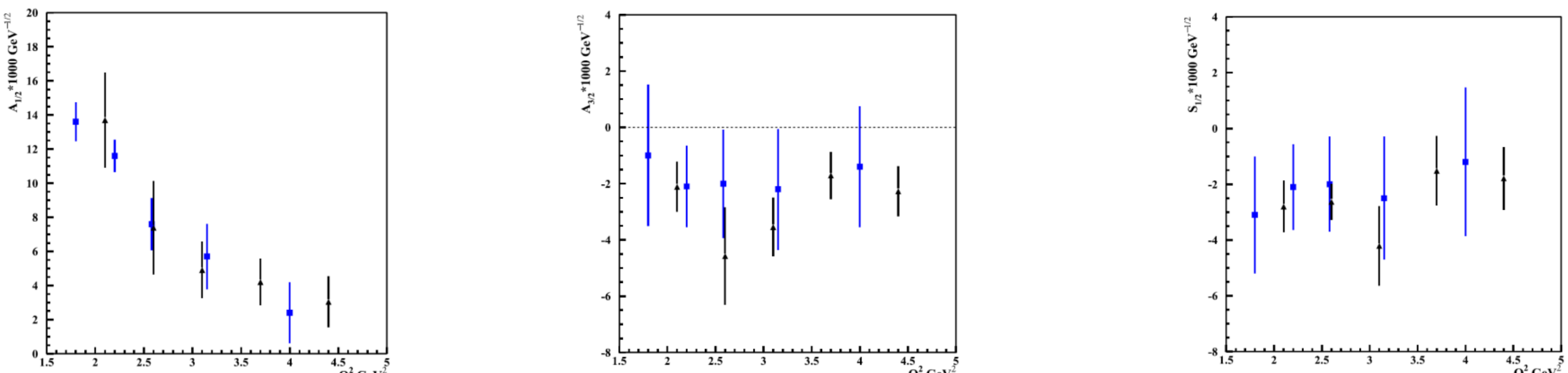

Also consistent with previously fixed hadronic parameter for M_{N*} >1.65 PRC 108, 025204 (2023) as well as independent analyses from the Nπ differential cross sections PRC 91, 045203 (2015) .

Conclusion

Emergence of Hadron Mass and Structure

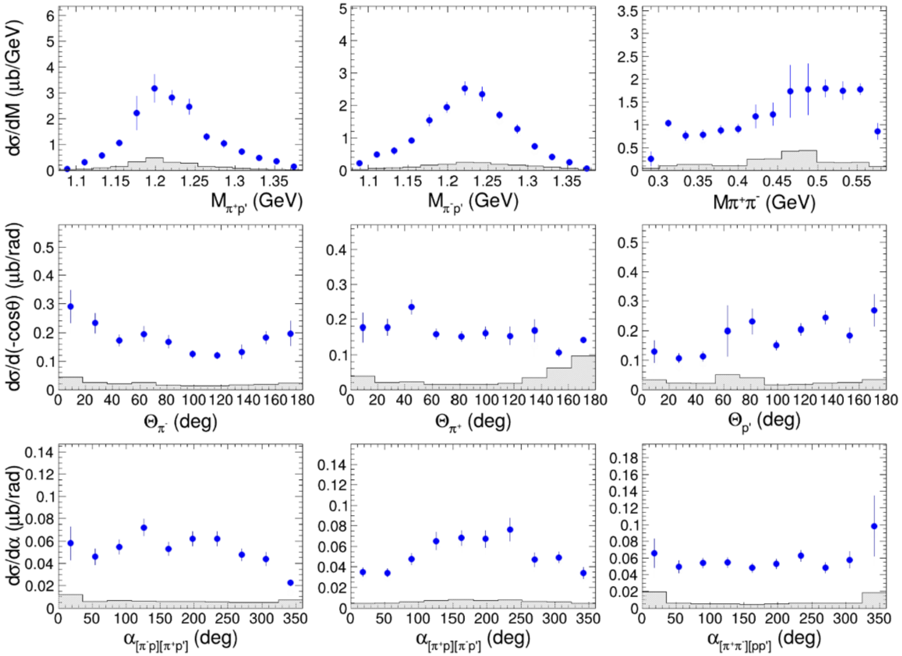

final cross sections

CLAS12

$W \in [1.50, 1.55]$ GeV
$Q^2 \in [6.0, 7.0]$ GeV^2

systematic uncertainties

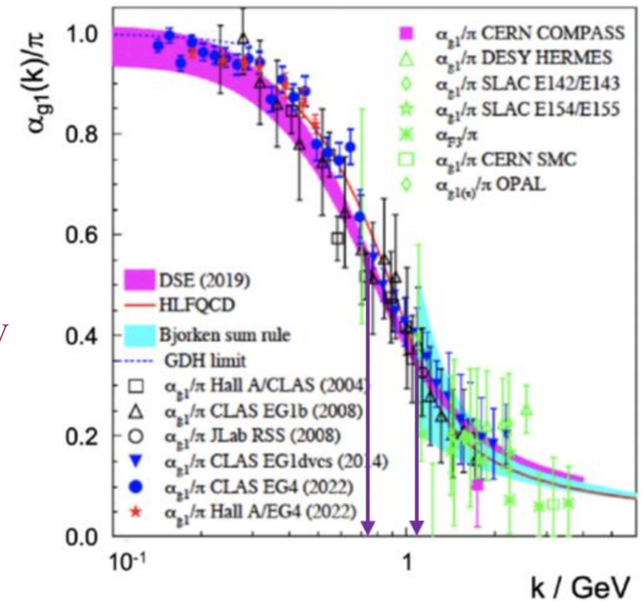

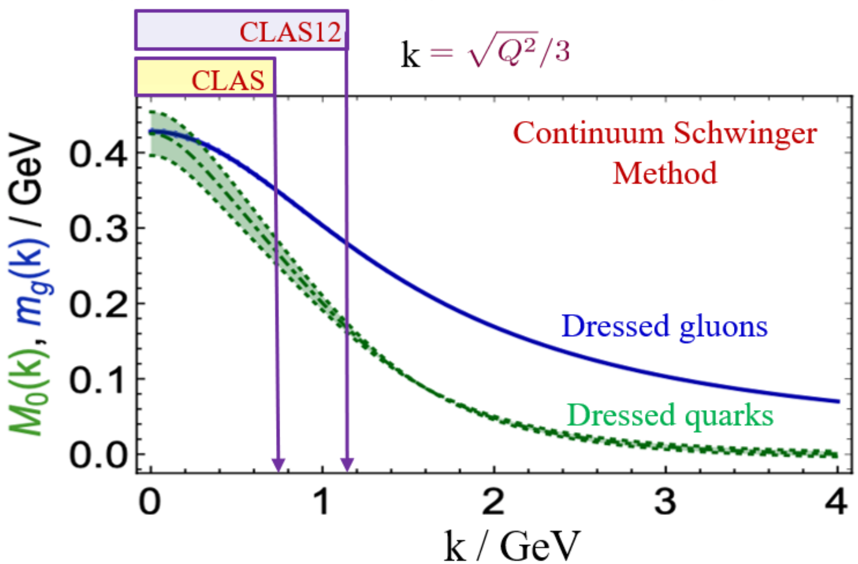

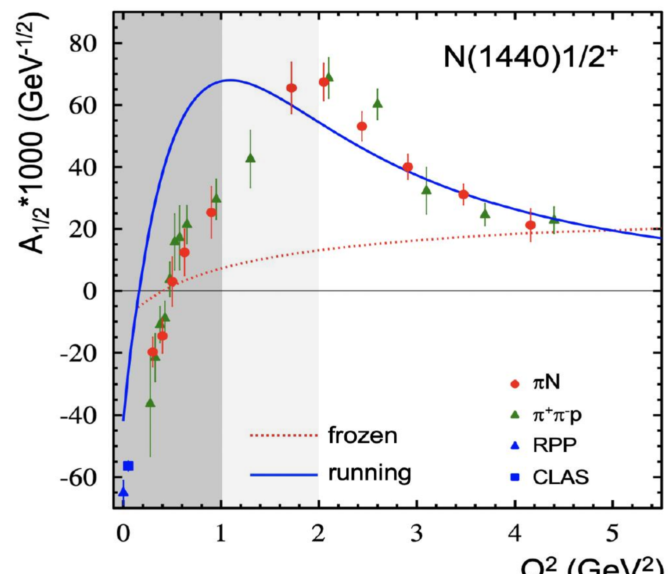

Beam Time Needs for Exclusive $p\pi^+\pi^-$ at CLAS22

Alexis Osmond & Krishna Neupane

Based on RGA Fall 2018 Luminosity of 5.96 10^{34} cm^{-2} s^{-1} at 45 nA and 5 cm LH_2

Simulated at 22 GeV Beam Energy

Needed Years at $5.96\cdot10^{34}$ (cm^{-2} s^{-1})

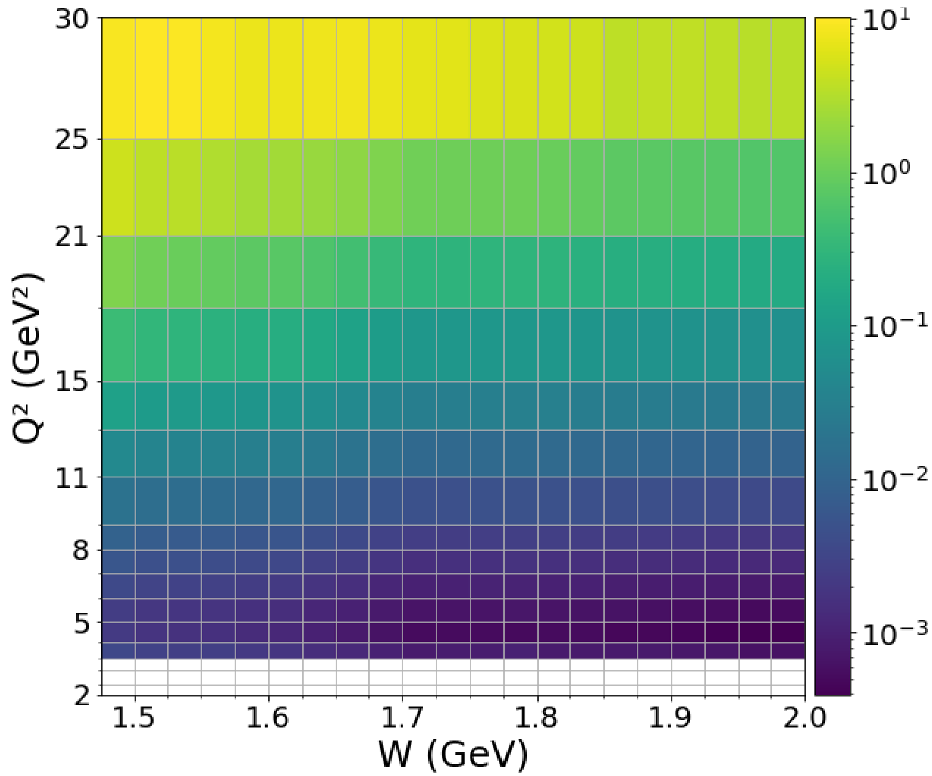

Simulated at 10.6 GeV Beam Energy

Needed Years at $5.96\cdot10^{34}$ (cm^{-2} s^{-1})

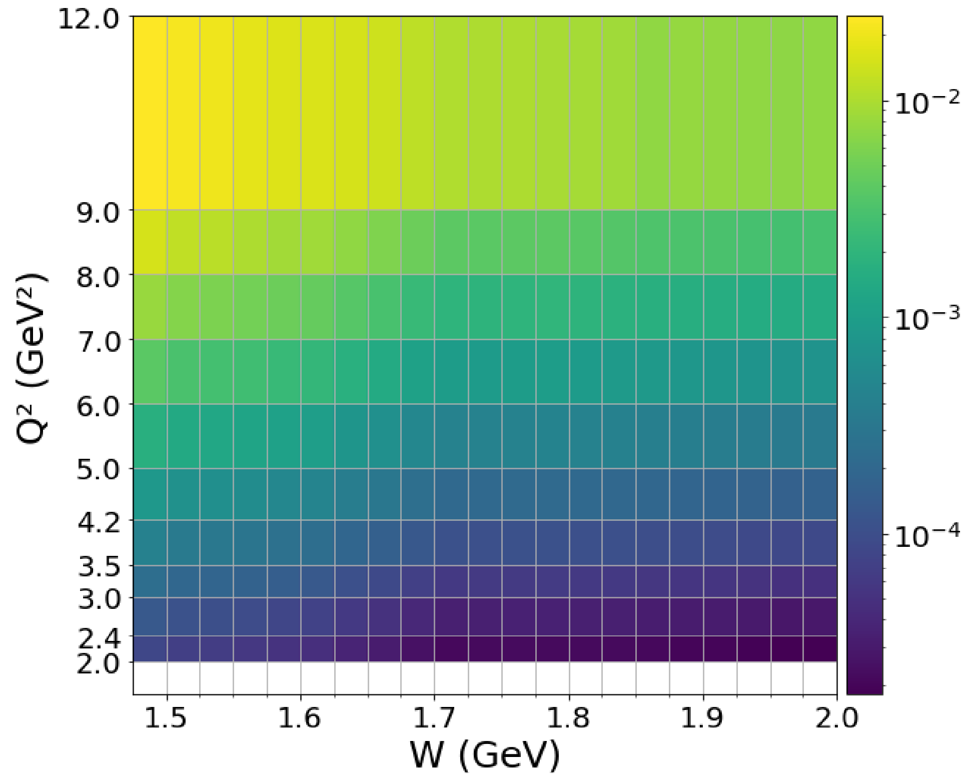

Implementing all analysis cuts (3/2), Golden Run Selection (3), PAC Days (2)

➡ 8 (16) years at $5.96\cdot10^{34}$ cm^{-2} s^{-1} or 11 (22) month at $5\cdot10^{35}$ cm^{-2} s^{-1}

Emergence of Hadron Mass and Structure

	Q^2-coverage of electrocouplings	Range of quark momenta k	Fraction of dressed quark mass at $k<k_{max}$
CLAS	< 5 GeV^2	< 0.8 GeV	30%
CLAS12	< 12 GeV^2	< 1.2 GeV	50%
CLAS22	< 35 GeV^2	< 2.0 GeV	90%

- Beam energy 22 GeV
- Nearly 4π acceptance

Increasing knowledge on running dressed quark mass from the results on $\gamma_v pN^*$ electrocouplings.

Measured $\gamma_v pN^*$ electrocouplings of most prominent N* states of different structure will provide sound evidence for understanding how the dominant part of the hadron mass and the N* structure itself emerge from QCD and will make CEBAF@22 GeV the ultimate QCD-facility at the luminosity frontier.

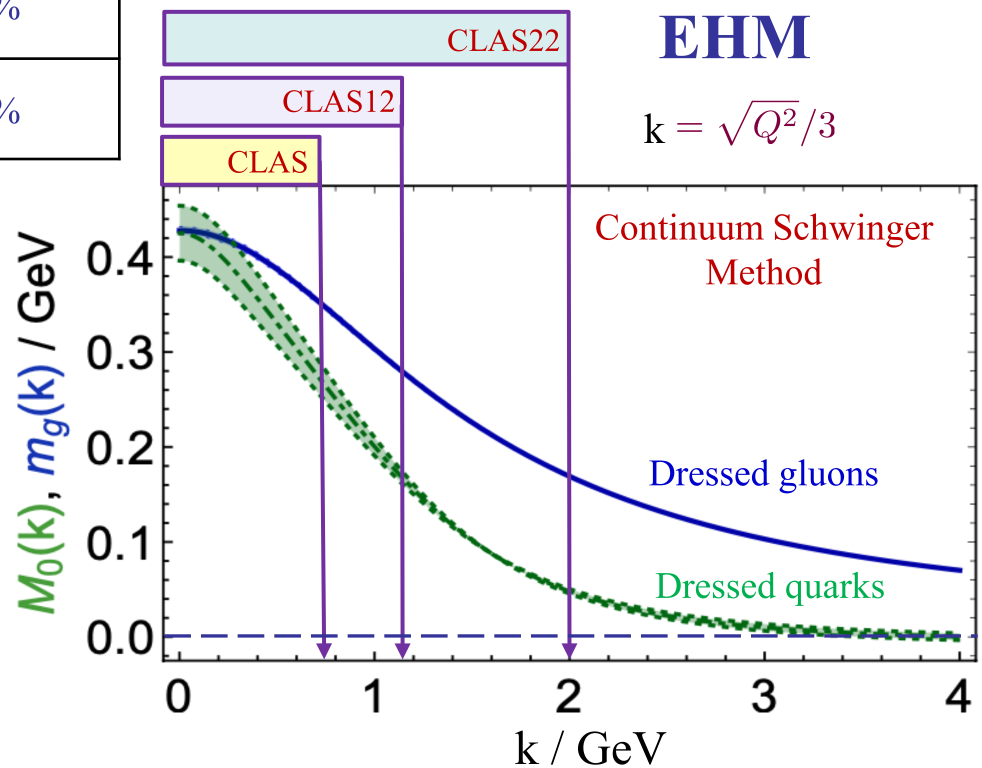

Luminosity "frontier" is the *unique* advantage of JLab.

Emergence of Hadron Mass and Structure

	Q^2-coverage of electrocouplings	Range of quark momenta k	Fraction of dressed quark mass at $k<k_{max}$
CLAS	< 5 GeV^2	< 0.8 GeV	30%
CLAS12	< 12 GeV^2	< 1.2 GeV	50%
CLAS22	< 35 GeV^2	< 2.0 GeV	90%

- Beam energy 22 GeV
- Nearly 4π acceptance

Increasing knowledge on running dressed quark mass from the results on $\gamma_v pN^*$ electrocouplings.

Measured $\gamma_v pN^*$ electrocouplings of most prominent N* states of different structure will provide sound evidence for understanding how the dominant part of the hadron mass and the N* structure itself emerge from QCD and will make CEBAF@22 GeV the ultimate QCD-facility at the luminosity frontier.

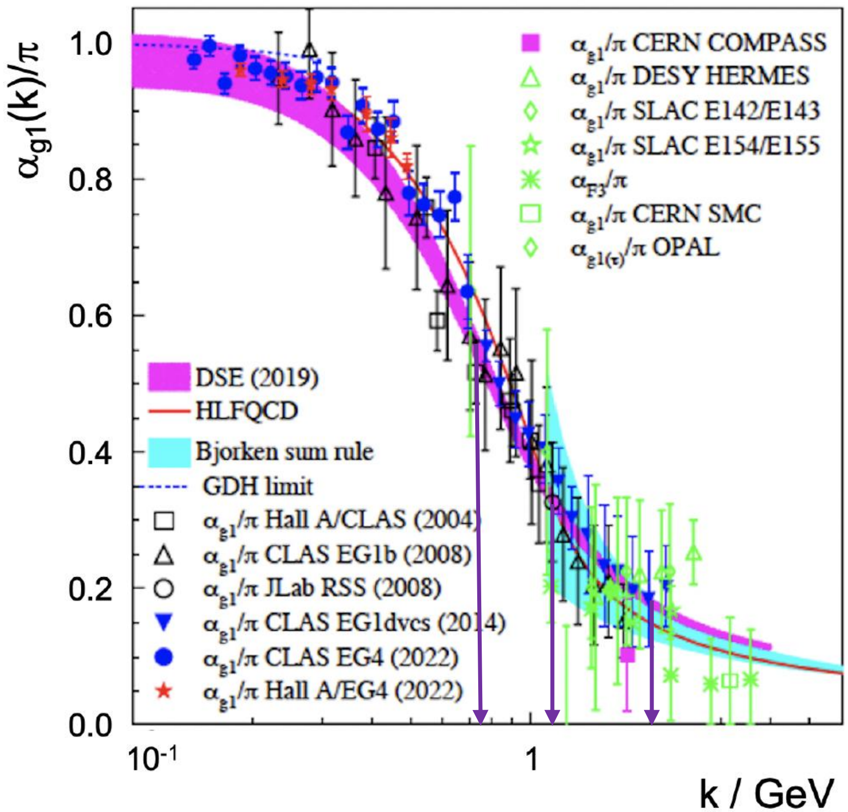

Luminosity "frontier" is the *unique* advantage of JLab.

JLab @ 22 GeV and EHM

e-Print: 2306.09360
E.P.J. A 60 (2024) 9, 173

Strong Interaction Physics at the Luminosity Frontier
with 22 GeV Electrons at Jefferson Lab

A. Accardi[1], P. Achenbach[2], D. Adhikari[3], A. Afanasev[4], C.S. Akondi[5], N. Akopov[6],
M. Albaladejo[7], H. Albataineh[8], M. Albrecht[2], B. Almeida-Zamora[9], M. Amaryan[10],
D. Androić[11], W. Armstrong[12], D.S. Armstrong[13], M. Arratia[14], J. Arrington[15],
A. Asaturyan[16], A. Austregesilo[2], H. Avagyan[2,*], T. Averett[13], C. Ayerbe Gayoso[13],
A. Bacchetta[17], A.B. Balantekin[18], N. Baltzell[2], L. Barion[19], P. C. Barry[2], A. Bashir[20,2],
M. Battaglieri[21], V. Bellini[22], I. Belov[21], O. Benhar[23], B. Benkel[24], F Benmokhtar[25],
W. Bentz[26], V. Bertone[27], H. Bhatt[28], A. Bianconi[29], L. Bibrzycki[30], R. Bijker[31],
D. Binosi[32], D. Biswas[3], M. Boër[3], W. Boeglin[33], S.A. Bogacz[2,*], M. Boglione[34],
M. Bondí[22], E.E. Boos[35], P. Bosted[13], G. Bozzi[36], E.J. Brash[37], R. A. Briceño[38],
P.D. Brindza[10], W.J. Briscoe[4], S.J Brodsky[39], W.K. Brooks[40,41,42], V.D. Burkert[2],
A. Camsonne[2], T. Cao[2], L.S. Cardman[2], D.S. Carman[2], M Carpinelli[43], G.D. Cates[44],

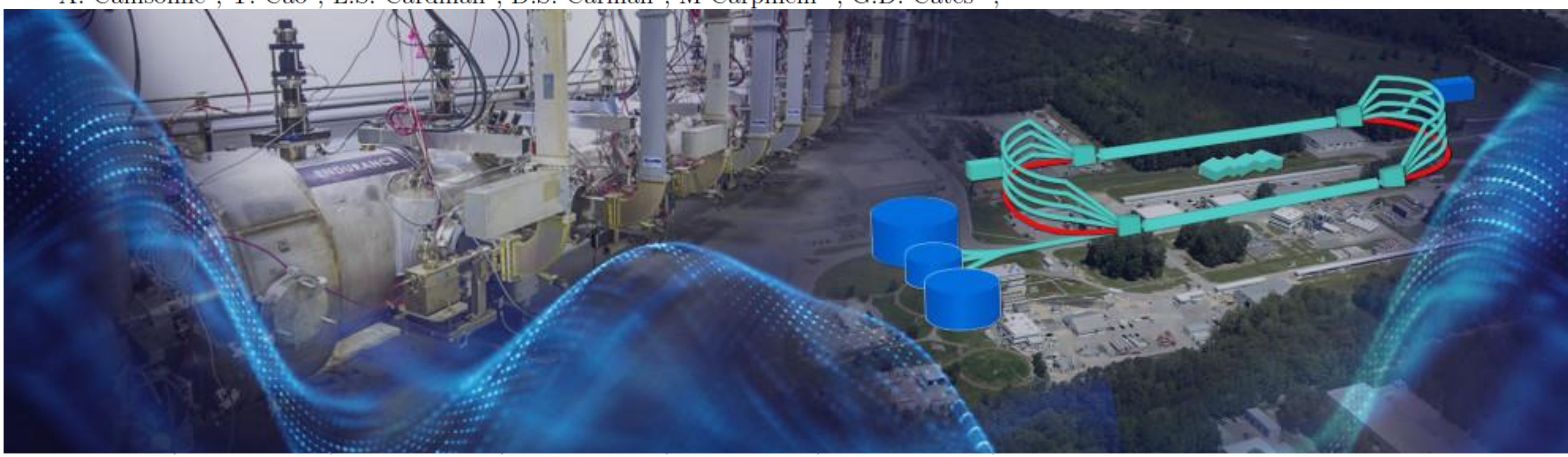

G.-P. Gilfoyle[87], F-X Girod[2], D. I. Glazier[84], C. Gleason[88], S. Godfrey[89], J.L. Goity[2,1],
A.A. Golubenko[35], S. Gonzàlez-Solís[90], R.W. Gothe[91,*], Y. Gotra[2], K. Griffioen[13],
O. Grocholski[92], B. Grube[2], P. Guèye[79], F.-K. Guo[93,94], Y. Guo[95], L. Guo[33], T. J. Hague[15],
N. Hammoud[85], J.-O. Hansen[2], M. Hattawy[10], F. Hauenstein[2], T. Hayward[62], D. Heddle[37],
N. Heinrich[96], O. Hen[67], D.W. Higinbotham[2], I.M. Higuera-Angulo[97], A. N. Hiller Blin[98], …

* 16 editors
444 authors

JLab @ 22 GeV and EHM

Strong Interaction Physics at the Luminosity Frontier
with 22 GeV Electrons at Jefferson Lab

e-Print: 2306.09360
E.P.J. A 60 (2024) 9, 173

6.5 Bound Three-Quark Structure of Excited Nucleons and Emergence of Hadron Mass

D.S. Carman, R.W. Gothe, V.I. Mokeev, C.D. Roberts

6.5.1 The Emergent Hadron Mass Paradigm

The Standard Model of Particle Physics has one well-known mass-generating mechanism for the most elementary constituents of Nature, *viz.* the Higgs boson [295, 296], which is critical to the evolution of the Universe. Yet, alone, the Higgs is responsible for just 1% of the visible mass in the Universe. Visible matter is constituted from nuclei found on Earth and the mass of each such nucleus is largely the sum of the masses of the nucleons they contain. However, only 9 MeV of a nucleon's mass, $m_N = 940$ MeV, is directly generated by Higgs boson couplings into quantum chromodynamics (QCD). Evidently, as highlighted by Fig. 46, Nature has another, very effective, mass-generating mechanism. Often called emergent hadron mass (EHM) [202, 297–299], it is responsible for 94% of m_N, with the remaining 5% generated by constructive interference between EHM and the Higgs boson. This makes studies of the structure of ground and excited nucleon states in experiments with electromagnetic probes a most promising avenue to gain insight into the strong interaction dynamics that underlie the emergence of the dominant part of the visible mass in the Universe [105, 202, 300–302].

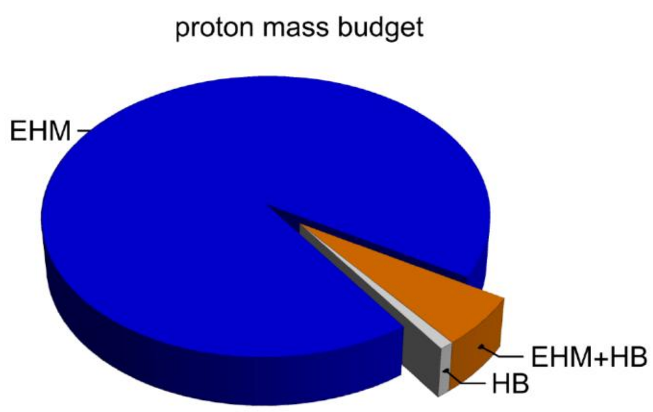

Figure 46: Proton mass budget, drawn using a Poincaré-invariant decomposition: emergent hadron mass (EHM) = 94%; Higgs boson (HB) contribution = 1%; and EHM+HB interference = 5%. (Separation at renormalization scale $\zeta = 2$ GeV, calculated using information from Refs. [22, 303–305]).

* 16 editors
444 authors

…